

# Tracking Control of Wheeled Mobile Robots Using Fuzzy CMAC Neural Networks

Ter-Feng Wu

Department of Electrical Engineering, National Ilan University, Taiwan  
tfwu@niu.edu.tw

## Abstract

This paper investigates the trajectory tracking control problem of wheeled mobile robots. First, the analytic B-spline function is used to generate a smooth feasible trajectory between the initial and the desired configurations so that the motion path can pass through the desired intermediate points to satisfy the kinematic constraints and curvature restrictions. Given the desired B-spline trajectory, the corresponding reduced dynamics can be used to design the control law for the privileged coordinates. Although the privileged coordinates can be driven to the desired values, the postured coordinates may significantly deviate from the reference values if the initial conditions are not appropriately provided, or there are disturbances during the motion. To solve this problem, the fuzzy control results are presented from the practical experience of driving to steer the postured coordinates in a kinematic level. To enhance the robot tracking performance and assure the error convergence, the robust adaptation laws for the FCMAC and compensated controller are derived from the stability analysis. Finally, an illustrated example shows the performance of the proposed trajectory tracking robot control scheme.

**Keywords:** Tracking control, Mobile robot, B-spline function, Fuzzy control, FCMAC

## 1 Introduction

The purpose of motion planning is to generate a reasonable path that can connect the initial posture (i.e., the position and orientation of the robot) and the final one so that no collisions with obstacles would occur and the kinematic constraints are satisfied. *B*-spline curves [1-4] have completed properties, such as having a small set of control points, being locally refined without changing their global shape, and having a convex hull, which make them suitable for representation forms in trajectory planning [5-6]. Nonholonomic properties most commonly appear in mechanical systems where the non-integration constraints are imposed on the motions. The non-integration of the nonholonomic constraints makes the tracking control

of mobile robots [7-8] with rolling and non-slipping wheels notably difficult. With Brockett's necessary stability conditions [9-10], a nonholonomic system with the under-actuated property cannot be asymptotically stabilized to a desired configuration using any smooth time-invariant state feedback. Alternatively, the kinematic equations are sometimes treated as a control problem, and one attempts to design the so-called kinematic controller, where the discontinuous feedback [11-12], time-varying feedback [13], hybrid feedback [14], sliding-mode control [15] and feedback linearization [16] may be used. However, the control for a kinematical model usually ignores the mass and inertia of the physical systems. The control inputs of the kinematics do not concern the actual applied force or torque with no physical significance; thus, the designs are considered impractical. Therefore, developing a complete controller structure for the nonholonomic systems should simultaneously consider the kinematic model and dynamic model. Fierro and Lewis [17] integrated a kinematic controller and a torque controller to stabilize a nonholonomic mobile robot, where there was the system uncertainty. Ge and Zhou [18] and Dong and Huo [19] investigated the point stabilization problems for the uncertain dynamic model and kinematic skew symmetric chained form of the wheeled mobile robot; then, they designed the adaptive controller for the combined system. An intelligent controller is considered an effective tool for wheeled mobile robots, where neuron-based adaptive control [20], GA (genetic algorithms) [21-22] based fuzzy control [23-24], and EP (evolutionary programming)-based kinematic control were studied.

In this paper, we use the cubic *B*-spline function to plan the trajectory of the mobile robot. We apply the constrained optimization method to solve the control points of the *B*-spline curve so that the motion path can pass through the desired intermediate points and satisfy the kinematic constraints and curvature restrictions. Next, we develop a feasible and practical methodology of controller design, which appropriately accommodates the dynamics and kinematic constraints. The adaptive fuzzy cerebellar model arithmetic controller (FCMAC) is considered in the dynamical

level, where the dynamic parameters of the mobile robot are supposed to be uncertain. The practical experience of driving can be embedded in the fuzzy logic-based system in the kinematical level. A fuzzy rule mechanism is established to compensate the desired values of the privileged coordinates. A new set of reference values for the privileged coordinates is computed; then, the FCMAC controller in the dynamical level is invoked to track the new reference, which in turn drives the postured coordinates to the desired B-spline curve. By [25], our proposed methods can be applied to dealing with text strings in the future work. Text strings are widely used as identifiers in our daily lives, such as Internet access accounts and passwords, email addresses, car license plates and credit cards. When a group of identifiers is associated with a certain characteristic, it becomes imperative to find out whether a random identifier belongs to this group for some applications. The objective of the proposed scheme is to achieve prompt responses, indicating membership of a query string and its associative attributes at the same time.

The remainder of this paper is organized as follows. In Section 2, we describe the practical problem of tracking a desired trajectory for a three-wheeled mobile robot. In Section 3, the trajectory-planning problem can be converted into a constrained optimization problem, and the control points of the B-spline curve can be solved by means of the constrained optimization algorithm. We use the fuzzy logic system to design the compensated value of the privileged velocities, and the adaptive FCMAC is developed for the dynamical model. Simulation examples are presented in Section 4. Finally, some concluding comments on the trajectory-tracking problem are provided in Section 5.

## 2 Motion Equations for Mobile Robots

The variables in this paper are listed in the Appendix A. The practical problem to be solved in this paper is the tracking of a desired trajectory for a three-wheeled mobile robot, whose configuration is shown in Figure 1. Let us consider the mobile robot that moves on a horizontal plane, which is driven by two actuated wheels with fixed orientation and supported by a castor wheel with varying orientation, as shown in Figure 2. The system may be modeled by a platform (body  $p$ ) with mass  $m_p$ , width  $\bar{b}$  and length  $l$ , attached to two rolling-without-sliding wheels (bodies 1 & 2) of identical mass  $m_w$  and radius  $a$ . The masses of the rim of each wheel and platform are denoted by  $m'_w$  and  $m'_p$ , respectively. Let  $b$  denote the width of the two wheels and  $\rho_r$  be the distance between point  $Q_r$  and the mass center of platform  $C_p$ .

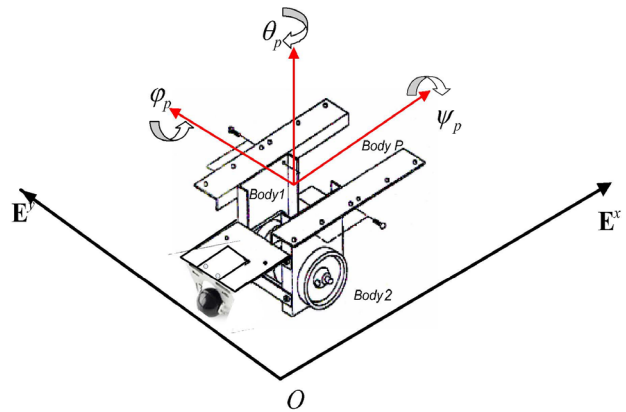


Figure 1. A three-wheeled mobile robot

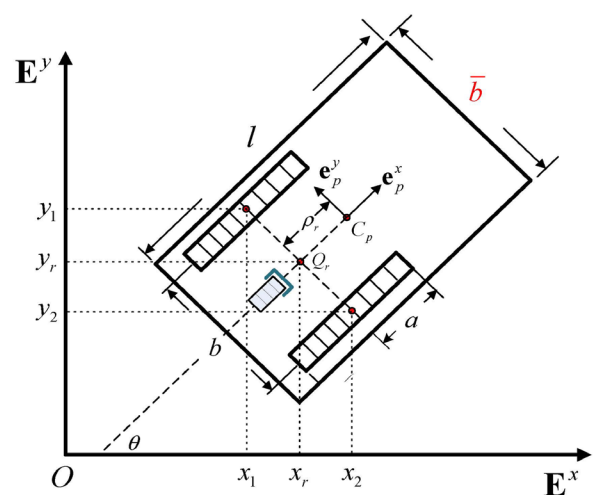


Figure 2. Configuration of the mobile robot

### 2.1 Kinematic Equation of the Wheeled Mobile Robots

Six variables  $(x_i, y_i, z_i, \theta_i, \psi_i, \phi_i, i=1, 2, p)$  are used here to describe the configuration of body  $i$ . Therefore, there are generally eighteen variables to be specified for the system. However, because of the physical constraints, the number may be reduced. Assuming that the motion is horizontal, we have (i)  $z_1 = a$ ; (ii)  $z_2 = a$ ; (iii)  $z_p = h_p$ . The platform is assumed to remain horizontal so that (iv)  $\phi_p = 0$  and (v)  $\psi_p = 0$ . If the wheels are properly aligned, the camber angles for the wheels vanish: (vi)  $\psi_1 = 0$ ; (vii)  $\psi_2 = 0$ . Moreover, if the steering mechanism is set, we impose additional constraints on the heading angles: (viii)  $\theta_1 = \theta_2 (\equiv \theta)$ ; (ix)  $\theta_2 = \theta_p$ . From the geometry of the interconnected bodies (Figure 2), we have the last four geometric constraints:

$$\begin{aligned}
 (x) \quad & x_2 = x_1 + 2b \sin \theta, \\
 (xi) \quad & y_2 = y_1 - 2b \cos \theta, \\
 (xii) \quad & x_p = x_1 + b \sin \theta + \rho_r \cos \theta, \\
 (xiii) \quad & y_p = y_1 - b \cos \theta + \rho_r \sin \theta.
 \end{aligned} \tag{1}$$

Finally, the wheels roll without sliding or slipping, which is realized by the following constraints:

$$\begin{aligned}\dot{x}_1 &= a\dot{\phi}_1 \cos \theta_1, \\ \dot{y}_1 &= a\dot{\phi}_1 \sin \theta_1, \\ \dot{x}_2 &= a\dot{\phi}_2 \cos \theta_2, \\ \dot{y}_2 &= a\dot{\phi}_2 \sin \theta_2.\end{aligned}\quad (2)$$

Because of the geometric constraint (viii), the previous four kinematic constraints (2) can be converted to the following three independent constraints:

$$\begin{aligned}(xiv) \quad \dot{x}_1 \cos \theta + \dot{y}_1 \sin \theta &= a\dot{\phi}_1, \\ (xv) \quad \dot{x}_1 \sin \theta - \dot{y}_1 \cos \theta &= 0, \\ (xvi) \quad a\dot{\phi}_1 + 2b\dot{\theta} &= a\dot{\phi}_2\end{aligned}\quad (3)$$

Condition (xvi) can be integrated to a geometric condition: (xvi')  $a\phi_1 + 2b\theta = a\phi_2 + (\text{a constant})$ . However, Conditions (xiv) and (xv) are not integrated, so the system is subject to two nonholonomic constraints.

Now, we derive the kinematic equations for the system of a wheeled mobile robot as shown in Figure 2. To describe the motion in terms of the coordinates of  $Q_r$  (the centers of the left and right wheels),  $x_r = x_1 + b \sin \theta$  and  $y_r = y_1 - b \cos \theta$  are used. We have

$$\begin{aligned}\dot{x}_r \cos \theta + \dot{y}_r \sin \theta - a\dot{\phi}_1 - b\dot{\theta} &= 0, \\ \dot{x}_r \sin \theta - \dot{y}_r \cos \theta &= 0\end{aligned}\quad (4)$$

We transform the above equations into the matrix form  $\mathbf{D}\dot{\mathbf{q}}=0$ , where the generalized coordinate  $\mathbf{q}=[x_r, y_r, \phi_1, \theta]^T$  and two nonholonomic conditions (xiv) and (xv) may be rewritten in the form of a  $2 \times 4$  coefficient matrix  $\mathbf{D}$

$$\mathbf{D} = \begin{pmatrix} \cos \theta & \sin \theta & -a & -b \\ \sin \theta & -\cos \theta & 0 & 0 \end{pmatrix}\quad (5)$$

The variable  $\theta$  appears in the elements of  $\mathbf{D}$ ; hence, it must be selected as a privileged coordinate; otherwise, the dynamical system may not be reducible. The other independent privileged velocity is  $\dot{\phi}_1$ , on which the control torque  $\tau_1$  directly acts, i.e.,  $\mathbf{u}=(\dot{\phi}_1, \dot{\theta})$ . The kinematic equation  $\dot{\mathbf{q}}=\mathbf{A}\mathbf{u}$  for the non-privileged velocities  $\dot{x}_r$  and  $\dot{y}_r$  can be derived with coefficient matrix  $\mathbf{A}$

$$\mathbf{A} = \begin{pmatrix} a \cos \theta & a \sin \theta & 1 & 0 \\ b \cos \theta & b \sin \theta & 0 & 1 \end{pmatrix}^T\quad (6)$$

Accordingly, in terms of  $u_1 = \dot{\phi}_1$  and  $u_2 = \dot{\theta}$ , the kinematic equation  $\dot{\mathbf{q}}=\mathbf{A}\mathbf{u}$  of the three-wheeled mobile robots can be expressed as

$$\dot{x}_r = (au_1 + bu_2) \cos \theta, \quad \dot{y}_r = (au_1 + bu_2) \sin \theta, \quad \dot{\phi}_1 = u_1, \quad \dot{\theta} = u_2 \quad (7)$$

## 2.2 Dynamic Equation of Wheeled Mobile Robots

According to Tsai [26], we have the dynamical equations of the following form

$$\begin{bmatrix} M_{11} & M_{12} \\ M_{21} & M_{22} \end{bmatrix} \begin{bmatrix} \ddot{\phi}_1 \\ \ddot{\theta} \end{bmatrix} + \begin{bmatrix} C_{11} & C_{12} \\ C_{21} & C_{22} \end{bmatrix} \begin{bmatrix} \dot{\phi}_1 \\ \dot{\theta} \end{bmatrix} = \begin{bmatrix} B_{11} & B_{12} \\ B_{21} & B_{22} \end{bmatrix} \begin{bmatrix} \tau_1 \\ \tau_2 \end{bmatrix}. \quad (8)$$

Taking the state variables  $x_1 = \phi_1$ ,  $x_2 = \dot{\phi}_1$ ,  $x_3 = \theta$ ,  $x_4 = \dot{\theta}$ , ( $x_1$ : the left wheel's rotational position,  $x_2$ : the left wheel's rotational velocity,  $x_3$ : the heading angles,  $x_4$ : the heading angles velocity) the dynamical equation may be changed into the following form

$$\dot{\mathbf{x}} = \mathbf{F}(\mathbf{x}) + \mathbf{G}(\mathbf{x})\boldsymbol{\tau}, \quad (9)$$

where

$$\mathbf{F}(\mathbf{x}) = \begin{bmatrix} x_2 \\ -\bar{M}_{11}(C_{11}x_2 + C_{12}x_4) - \bar{M}_{12}(C_{21}x_2 + C_{22}x_4) \\ x_4 \\ -\bar{M}_{21}(C_{11}x_2 + C_{12}x_4) - \bar{M}_{22}(C_{21}x_2 + C_{22}x_4) \end{bmatrix}, \quad (10)$$

$$\mathbf{G}(\mathbf{x}) = \begin{bmatrix} 0 & 0 \\ \bar{M}_{11}B_{11} + \bar{M}_{12}B_{21} & \bar{M}_{11}B_{12} + \bar{M}_{12}B_{22} \\ 0 & 0 \\ \bar{M}_{21}B_{11} + \bar{M}_{22}B_{21} & \bar{M}_{21}B_{12} + \bar{M}_{22}B_{22} \end{bmatrix}, \quad (11)$$

$$\text{and } \begin{bmatrix} M_{11} & M_{12} \\ M_{21} & M_{22} \end{bmatrix}^{-1} = \begin{bmatrix} \bar{M}_{11} & \bar{M}_{12} \\ \bar{M}_{21} & \bar{M}_{22} \end{bmatrix}.$$

The details can be referred to Tsai [26].

## 3 Design of the Controller

Let us consider the hierarchical model constructed by an under-actuated kinematical equation and a dynamical equation (9). The structure of the developed methodology consists of the adaptive FCMAC controller in the dynamical level and fuzzy logic compensator in the kinematical level. The objective of the design is to obtain a hierarchical controller that enables the system to track a reference  $B$ -spline trajectory and satisfies the geometric and kinematic constraints. Here, the adaptive controller is used because it can address the parameter uncertainties so that the privileged velocities ( $\mathbf{u}=[v, w]$ ) can be stabilized to the desired values. However, this effort does not guarantee the convergence of the position and orientation ( $\boldsymbol{\xi}=[x, y, \theta]$ ) of the mobile robot to the desired values if the initial postured coordinates are not appropriately set or there are some disturbances during the motion. To overcome this problem, we propose a fuzzy logic system to reason the compensated values

for the desired privileged velocities from the kinematics. A new set of reference values for the privileged velocities is obtained. Then, the mentioned adaptive FCMAC controller is invoked to track the new reference, which steers the postured coordinates to the desired values and control the *B*-spline trajectory tracking. The block diagram of the proposed control structure for the trajectory-tracking task is shown in Figure 3.

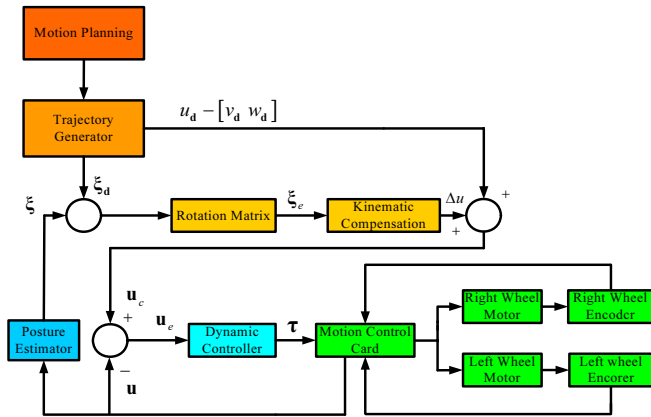


Figure 3. Block diagram of the *B*-spline tracking control

### 3.1 Fuzzy Logic Compensator in the Kinematical Level

Consider the following fuzzy logic system:

$$R_i : \text{IF } d_e = A_i \text{ and } \theta_e = B_i \text{ and } \vartheta_e = C_i \\ \text{THEN } \Delta v = D_i, \Delta w = E_i$$

where  $A_i, B_i, C_i, D_i$  and  $E_i$  are fuzzy sets for the  $i$ th rule;  $d_e$  is the error distance between the current position and the desired position;  $\theta_e$  is the error angle between the current and the desired heading angles;  $\vartheta_e$  is the orientation angle from the current position to the desired position;  $\Delta v$  and  $\Delta w$  are the compensated values of the linear velocity and angular velocity of the vertical axis at point  $Q$  of the rear wheels, respectively. We define the posture error vector  $\xi_e$  in the body frame as a coordinate transformation of the difference between the desired and the current postures in the inertial frame, which is described in Figure 4.

$$\begin{bmatrix} x_e \\ y_e \\ \theta_e \end{bmatrix} = \begin{bmatrix} \cos \theta & \sin \theta & 0 \\ -\sin \theta & \cos \theta & 0 \\ 0 & 0 & 1 \end{bmatrix} \begin{bmatrix} x_d - x \\ y_d - y \\ \theta_d - \theta \end{bmatrix}, \quad (12)$$

where

$$\begin{aligned} x_e &= \cos(x_d - x) + \sin(y_d - y), \\ y_e &= -\sin(x_d - x) + \cos(y_d - y), \\ \theta_e &= \theta_d - \theta. \end{aligned}$$

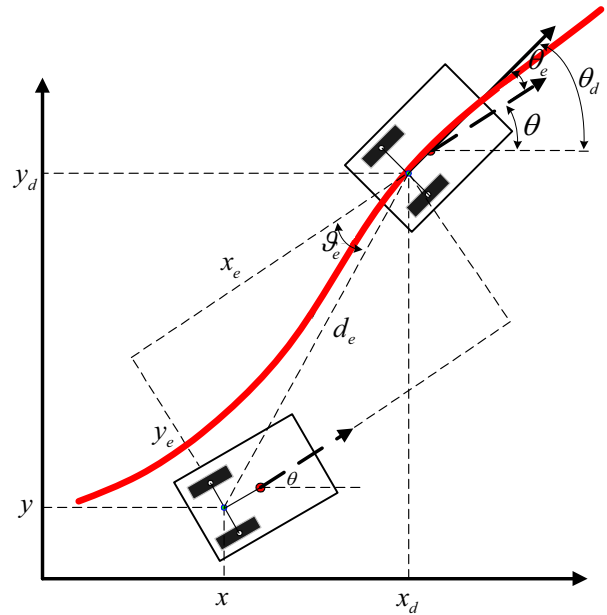


Figure 4. Error configuration in the body frame

$x, y, \theta$  is the current position,  $x_d, y_d, \theta_d$  is the desired position. The distance from the current position to the desired position is denoted by  $d_e = \sqrt{x_e^2 + y_e^2}$ , and the corresponding orientation angle is expressed as  $\vartheta_e = \tan^{-1} \frac{y_e}{x_e}$ , which shall be termed the path angle and is different from the heading angle error  $\theta_e$ . The kinematic compensator is established which adopt the idea of fuzzy logic system based on human knowledge and experiences. The sets of input variables of the fuzzy system are chosen as  $(d_e, \vartheta_e, \theta_e)$ .

To improve the tracking performance, we incorporate three input variables ( $d_e = \sqrt{x_e^2 + y_e^2}$ ,  $\theta_e = \theta_d - \theta$  and  $\vartheta_e = \tan^{-1} \left( \frac{y_e}{x_e} \right)$ ) into our antecedent part of the fuzzy rules, and the consequent part of the fuzzy rules generate two output variables  $\Delta u = [\Delta v, \Delta w]$ . Clearly, from this description, the magnitude of  $d_e$  is used to determine the compensated value of linear velocity  $\Delta v$ . For the compensated angular velocity  $\Delta w$ , two variables  $\theta_e$  and  $\vartheta_e$  should be simultaneously considered. If only  $\theta_e$  is considered, a desired tracking performance cannot be guaranteed for the mobile robot. It may go forward in parallel with the reference trajectory. However, if only  $\vartheta_e$  is considered, the compensated value  $\Delta w$  of the fuzzy inference will experience a high-frequency switch (chattering phenomenon) near the reference trajectory.

In this paper, the fuzzy logic compensation is proposed, which integrates the expert experiences into the design process using linguistic rules. The fuzzy set of linguistic values is denoted as follows:  $A_i = \{ZE, PS,$

PM, PB};  $B_i = \{PB, PM, PS, ZE, NS, NM, NB\}$ ;  $C_i = \{P, Z, N\}$ ;  $D_i = \{ZE, PS, PM, PB\}$ ;  $E_i = \{PB, PM, PS, ZE, NS, NM, NB\}$ .

Now, we specify seven linguistic values PB, PM, PS, ZE, NS, NM, and NB, which correspond to “Positive Big”, “Positive Medium”, “Positive Small”, “Zero”, “Negative Small”, “Negative Medium”, and “Negative Big”, respectively. The membership functions of the linguistic values and their ranges are shown in Figure 5, where the triangular, trapezoid and singleton are used to describe the antecedent and consequent fuzzy sets.

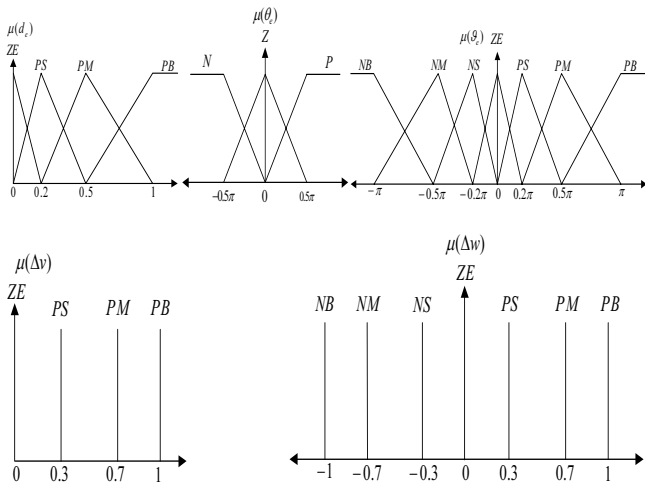


**Figure 5.** Membership functions of fuzzy sets  $A_i$ ,  $B_i$ ,  $C_i$ ,  $D_i$  and  $E_i$

**Table 1.** Table of fuzzy rules

$\theta_e$		$d_e$							
		ZE		PS		PM		PB	
$P$		$\Delta v$	$\Delta w$						
	$PB$	ZE	PB	ZE	PM	ZE	PS	ZE	ZE
$\mathcal{G}_e$	$PM$	ZE	PB	ZE	PM	ZE	PS	PS	ZE
	$PS$	ZE	PM	PS	PS	PS	ZE	PM	ZE
	$ZE$	ZE	PM	PS	ZE	PM	ZE	PB	ZE
	$NS$	ZE	PM	PS	NS	PS	ZE	PM	ZE
	$NM$	ZE	PS	ZE	NM	ZE	NS	PS	ZE
	$NB$	ZE	PS	ZE	NM	ZE	NS	ZE	ZE

$\theta_e$		$d_e$							
		ZE		PS		PM		PB	
$Z$		$\Delta v$	$\Delta w$						
	$PB$	ZE	ZE	ZE	PM	ZE	PS	ZE	ZE
$\mathcal{G}_e$	$PM$	ZE	ZE	PS	PM	PS	PS	PM	ZE
	$PS$	ZE	ZE	PS	PS	PM	ZE	PB	ZE
	$ZE$	ZE	ZE	PS	ZE	PM	ZE	PB	ZE
	$NS$	ZE	ZE	PS	NS	PM	ZE	PB	ZE
	$NM$	ZE	ZE	PS	NM	PS	NS	PM	ZE
	$NB$	ZE	ZE	ZE	NM	ZE	NS	ZE	ZE

$\theta_e$		$d_e$							
		ZE		PS		PM		PB	
$N$		$\Delta v$	$\Delta w$						
	$PB$	ZE	NS	ZE	PM	ZE	PS	ZE	ZE
$\mathcal{G}_e$	$PM$	ZE	NS	ZE	PM	ZE	PS	PS	ZE
	$PS$	ZE	NM	PS	PS	PS	ZE	PM	ZE
	$ZE$	ZE	NM	PS	ZE	PM	ZE	PB	ZE
	$NS$	ZE	NM	PS	NS	PS	ZE	PM	ZE
	$NM$	ZE	NB	ZE	NM	ZE	NS	PS	ZE
	$NB$	ZE	NB	ZE	NM	ZE	NS	ZE	ZE

Now, we denote  $\mathbf{u}_c = \mathbf{u}_d + \Delta \mathbf{u}$  as the new reference value for the privileged velocities. Then, the FCMAC in the dynamical level is invoked to track the new reference. It can enable the privileged velocities in the dynamical model to smoothly follow the new desired value of  $\mathbf{u}_c$ ; more importantly, it can make the posture coordinates  $\xi$  in the kinematical model simultaneously follow the desired trajectory.

### 3.2 Fuzzy CMAC Compensator in the Dynamical Level

#### (1) FCMAC

This section introduces the FCMAC. The basic

The fuzzy logic compensator is a rule-based system constructed from a collection of *IF-THEN* rules, which are designed based on human knowledge and experiences. We use straightforward ideas to constitute the inference mechanisms of the compensated linear velocity  $\Delta v$  and angular velocity  $\Delta w$ , and we provide the following tuning rules: ( $R_1$ ): *IF*  $d_e$  is close to zero, *THEN*  $\Delta v$  is close to zero; ( $R_2$ ): *IF*  $|\mathcal{G}_e|$  is large, *THEN*  $\Delta v$  is close to zero. ( $R_3$ ): *IF*  $|\mathcal{G}_e|$  or  $|\theta_e|$  gradually increases, *THEN* the compensated value  $\Delta v$  gradually decreases; ( $R_4$ ): *IF*  $\mathcal{G}_e$  is close to zero, *THEN*  $\Delta w$  is close to zero; ( $R_5$ ): *IF*  $d_e$  is large, *THEN*  $\Delta w$  is close to zero; ( $R_6$ ): *IF*  $d_e$  gradually increases, *THEN* the compensated value  $\Delta w$  gradually decreases. ( $R_7$ ): *IF*  $d_e$  is close to zero, *THEN* the compensated value  $\Delta w$  absolutely depends on  $\theta_e$ .

The fuzzy rule (Table 1) bases are given as follows. There are  $28 \times 3$  rules in total to decide the compensated values of the linear velocity and angular velocity of the wheeled mobile robots. The defuzzification process uses the center-of-gravity approach.

multivariable CMAC is designed to provide the output as

$$\mathbf{z}_{CMAC} = F(\mathbf{s})$$

where  $F: R^L \rightarrow R^m$  is a nonlinear function of the CMAC, the input variable is  $\mathbf{s} = [s_1 \ \dots \ s_L]^T \in S \subset R^L$  with the input space  $S$  and output variable  $\mathbf{z}_{CMAC} = [\mathbf{z}_{CMAC1} \ \dots \ \mathbf{z}_{CMACm}]^T \in Z \subset R^m$ . Figure 6 shows a simplified two-dimensional FCMAC. In the two-dimensional case, we can uniformly divide the bounded region into 4 elements:  $(-x, x)$  for variable  $s_1$  and  $(-y, y)$  for variable  $s_2$ . With this type of partition,

we have 16 labeled sub-regions in Figure 6. Each variable consists of three layers, and each layer contains two blocks. A block can accumulate some elements. For example, block D in the 2<sup>nd</sup> layer for input variable  $s_1$  accumulates elements  $x_2, x_3$  and  $x_4$ . However, block C contains only element  $x_1$ . Similarly, for input variables  $s_1$  and  $s_2$ , block f accumulates elements  $y_3$  and  $y_4$ . From the above descriptions, we have blocks A, B, C, D, E, F, a, b, c, d, e and f, i.e., 6 blocks {A, B, C, D, E, F} for input variable  $s_1$  and 6 blocks {a, b, c, d, e, f} for input variable  $s_2$ . The *receptive fields* are formed by the blocks and denoted as [Aa, Ab, Ba, Bb, Cc, Cd, Dc, Dd, Ee, Ef, Fe, Ff].

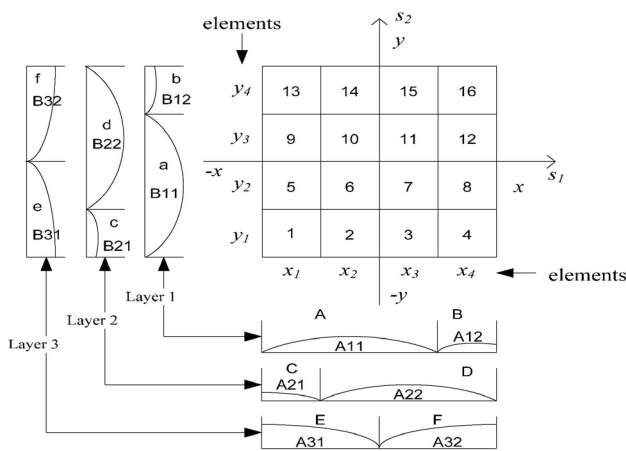


Figure 6. FCMAC architecture

The following Gaussian function is commonly used to describe the blocks and known as the *receptive-field functions*:

$$\phi(s) = e^{-\left[\frac{(s-m)^2}{\sigma^2}\right]}, \tag{13}$$

where  $m$  and  $\sigma$  are the mean and variance of the Gaussian function, respectively. Furthermore, the *multidimensional receptive-field functions* are represented by

$$\begin{aligned} &A(s_1)a(s_2), A(s_1)b(s_2), B(s_1)a(s_2), B(s_1)b(s_2), \\ &C(s_1)c(s_2), C(s_1)d(s_2), D(s_1)c(s_2), D(s_1)d(s_2), \\ &E(s_1)e(s_2), E(s_1)f(s_2), F(s_1)e(s_2), F(s_1)f(s_2). \end{aligned}$$

In Figure 6, we can assign a fuzzy set in each block, e.g., A11 for block A, A22 for block D, B32 for block f, and B21 for block c. The remaining fuzzy sets can be easily found from Figure 6. Therefore, we can describe the FCMAC system as a fuzzy system for each layer:

$(m,j,k)$ -rules: IF  $s_1 = A_{mj}$  and  $s_2 = B_{mk}$ , THEN  $y = w_{mj k}$ , where  $(m,j,k)$  denotes the  $m^{th}$  layer ( $m=1,2,3$ ), the  $j^{th}$  block for  $s_1$  ( $j=1,2$ ), the  $k^{th}$  block for  $s_2$  ( $k=1,2$ ) and weight  $w_{mj k}$ .

The multidimensional receptive-field function in this paper is defined by

$$\bar{\phi}_{mj k} = \frac{\phi_{mj k}}{\sum_{m=1}^{n_l} \sum_{j=1}^{n_B} \sum_{k=1}^{n_B} \phi_{mj k}} = \frac{\phi_{mj k}}{\sum_{m=1}^3 \sum_{j=1}^2 \sum_{k=1}^2 \phi_{mj k}}, \tag{14}$$

where  $n_l$  and  $n_B$  are the total number of layers and number of blocks in each layer, respectively, and

$$\phi_{mj k} = A_{mj}(s_1) \cdot B_{mk}(s_2), \tag{15}$$

$$A_{mj}(s_1) = e^{-\left[\frac{(s_1-m_{mj})^2}{\sigma_{mj}^2}\right]}, B_{mk}(s_2) = e^{-\left[\frac{(s_2-m_{mk})^2}{\sigma_{mk}^2}\right]}. \tag{16}$$

Finally, the output of the FCMAC is

$$\mathbf{z}_{CMAC} = \sum_{m=1}^3 \sum_{j=1}^2 \sum_{k=1}^2 \bar{\phi}_{mj k} w_{mj k} = \Phi \mathbf{w}, \tag{17}$$

where

$$\Phi = [\bar{\phi}_{111}, \bar{\phi}_{112}, \bar{\phi}_{121}, \bar{\phi}_{122}, \bar{\phi}_{211}, \bar{\phi}_{212}, \bar{\phi}_{221}, \bar{\phi}_{222}, \bar{\phi}_{311}, \bar{\phi}_{312}, \bar{\phi}_{321}, \bar{\phi}_{322}], \tag{18}$$

$$\mathbf{w} = [w_{111}, w_{112}, w_{121}, w_{122}, w_{211}, w_{212}, w_{221}, w_{222}, w_{311}, w_{312}, w_{321}, w_{322}]^T. \tag{19}$$

The weight vector  $\mathbf{w}$  of the FCMAC is adjustable.

Consider the following Multi-Input Multi-Output (MIMO) system:

$$\mathbf{y}^{(r)} = \mathbf{f}(\mathbf{x}) + \mathbf{G}(\mathbf{x})\mathbf{u} + \mathbf{d}(\mathbf{x}, t), \tag{20}$$

where  $\mathbf{r} = [r_1, r_2, \dots, r_m]$ ;  $\mathbf{y} = [y_1, y_2, \dots, y_m]^T$ ;  $\mathbf{y}^{(r)} = [y_1^{(r_1)}, y_2^{(r_2)}, \dots, y_m^{(r_m)}]^T$ ;  $\sum_{i=1}^m r_i = n$ ; the control input is

$$\begin{aligned} \mathbf{u} &= [u_1, u_2, \dots, u_m]^T; \text{ the state vector is} \\ \mathbf{x} &= [x_1, x_2, \dots, x_n]^T \\ &= [y_1, \dot{y}_1, \dots, y_1^{(r_1-1)}, y_2, \dot{y}_2, \dots, y_2^{(r_2-1)}, \dots, y_m, \dot{y}_m, \dots, y_m^{(r_m-1)}], \end{aligned} \tag{21}$$

nonlinear function vector  $\mathbf{f} = [f_1(\mathbf{x}), f_2(\mathbf{x}), \dots, f_m(\mathbf{x})]^T$ ; disturbance  $\mathbf{d}(\mathbf{x}, t) = [d_1(\mathbf{x}, t), d_2(\mathbf{x}, t), \dots, d_m(\mathbf{x}, t)]^T$ ; nonlinear function matrix

$$\mathbf{G}(\mathbf{x}) = [\mathbf{g}_1(\mathbf{x}), \mathbf{g}_2(\mathbf{x}), \dots, \mathbf{g}_m(\mathbf{x})]^T,$$

where

$$\mathbf{g}_i(\mathbf{x}) = [g_{i1}(x), g_{i2}(x), \dots, g_{im}(x)], \quad i = 1, 2, \dots, m \tag{22}$$

The MIMO system can be rewritten as

$$\begin{aligned} \begin{bmatrix} y_1^{(r_1)} \\ y_2^{(r_2)} \\ \vdots \\ y_m^{(r_m)} \end{bmatrix} &= \begin{bmatrix} f_1 \\ f_2 \\ \vdots \\ f_m \end{bmatrix} + \begin{bmatrix} \mathbf{g}_1 \\ \mathbf{g}_2 \\ \vdots \\ \mathbf{g}_m \end{bmatrix} \begin{bmatrix} u_1 \\ u_2 \\ \vdots \\ u_m \end{bmatrix} + \begin{bmatrix} d_1 \\ d_2 \\ \vdots \\ d_m \end{bmatrix} \\ &= \begin{bmatrix} f_1 \\ f_2 \\ \vdots \\ f_m \end{bmatrix} + \begin{bmatrix} g_{11} & g_{12} & \dots & g_{1m} \\ g_{21} & g_{22} & \dots & g_{2m} \\ \vdots & \vdots & \ddots & \vdots \\ g_{m1} & g_{m2} & \dots & g_{mm} \end{bmatrix} \begin{bmatrix} u_1 \\ u_2 \\ \vdots \\ u_m \end{bmatrix} + \begin{bmatrix} d_1 \\ d_2 \\ \vdots \\ d_m \end{bmatrix} \end{aligned} \tag{23}$$

In this paper, the control input is defined by

$$\mathbf{u} = (\bar{\mathbf{G}} + \hat{\mathbf{G}})^{-1} [-\bar{\mathbf{f}} - \hat{\mathbf{f}} + \mathbf{y}_d^{(r)} + \Lambda^T \mathbf{e} + \mathbf{u}_r], \quad (24)$$

where  $\mathbf{e}$  is the tracking error vector and defined as  $\mathbf{e} = [\mathbf{e}_1^T \mathbf{e}_2^T \cdots \mathbf{e}_m^T] \in R^n$ ;  $\mathbf{e}_i = [(\mathcal{Y}_{di} - \mathcal{Y}_i)(\dot{\mathcal{Y}}_{di} - \dot{\mathcal{Y}}_i) \cdots (\mathcal{Y}_{di}^{(r_i-1)} - \mathcal{Y}_i^{(r_i-1)})]$ ,  $i = 1, \dots, m$ ,  $\sum_{i=1}^m r_i = n$ .  $\Lambda$  is a designed positive constant matrix such that the tracking error vector will exponentially converge to an arbitrarily small residual set, where

$$\Lambda^T = \begin{bmatrix} \Lambda_1^T & \mathbf{0} & \cdots & \mathbf{0} \\ \mathbf{0} & \Lambda_2^T & \cdots & \mathbf{0} \\ \vdots & \vdots & \ddots & \vdots \\ \mathbf{0} & \mathbf{0} & \cdots & \Lambda_m^T \end{bmatrix} \in R^{m \times n}, \text{ and}$$

$$\Lambda_i^T = [-\lambda_{i1} \quad -\lambda_{i2} \quad \cdots \quad -\lambda_{ir_i}]$$

$\hat{\mathbf{G}} = \hat{\mathbf{G}}(\mathbf{x}|\mathbf{w})$  and  $\hat{\mathbf{f}} = \hat{\mathbf{f}}(\mathbf{x}|\mathbf{w})$  are constructed by FCMACs to estimate the system uncertainties [27];  $\bar{\mathbf{G}}$  and  $\bar{\mathbf{f}}$  are the nominal models;  $\mathbf{u}_r$  is the robust control vector;  $\mathbf{y}_d^{(r)}$  is the desired output vector. Applying the control input to the MIMO system, we have

$$\mathbf{y}_d^{(r)} - \mathbf{y}^{(r)} = \mathbf{e}^{(r)} = -\Lambda^T \mathbf{e} + (\bar{\mathbf{f}} + \hat{\mathbf{f}} - \mathbf{f}) + (\bar{\mathbf{G}} + \hat{\mathbf{G}} - \mathbf{G})\mathbf{u} - \mathbf{u}_r - \mathbf{d}, \quad (25)$$

where  $\hat{\mathbf{f}}$  and  $\hat{\mathbf{G}}$  are the uncertainties of dynamics, which are constructed by FCMACs to estimate the system uncertainties in this paper.

After some manipulations, we have

$$\begin{bmatrix} \dot{\mathbf{e}}_1 \\ \dot{\mathbf{e}}_2 \\ \vdots \\ \dot{\mathbf{e}}_m \end{bmatrix} = \begin{bmatrix} \mathbf{A}_1 & \mathbf{0} & \mathbf{0} & \mathbf{0} \\ \mathbf{0} & \mathbf{A}_2 & \mathbf{0} & \mathbf{0} \\ \mathbf{0} & \mathbf{0} & \ddots & \mathbf{0} \\ \mathbf{0} & \mathbf{0} & \mathbf{0} & \mathbf{A}_m \end{bmatrix} \begin{bmatrix} \mathbf{e}_1 \\ \mathbf{e}_2 \\ \vdots \\ \mathbf{e}_m \end{bmatrix} + \begin{bmatrix} \mathbf{b}_1 & \mathbf{0} & \mathbf{0} & \mathbf{0} \\ \mathbf{0} & \mathbf{b}_2 & \mathbf{0} & \mathbf{0} \\ \mathbf{0} & \mathbf{0} & \ddots & \mathbf{0} \\ \mathbf{0} & \mathbf{0} & \mathbf{0} & \mathbf{b}_m \end{bmatrix} \begin{bmatrix} (\bar{f}_1 + \hat{f}_1 - f_1) + (\bar{\mathbf{g}}_1 + \hat{\mathbf{g}}_1 - \mathbf{g}_1)u_1 - u_{r1} - d_1 \\ (\bar{f}_2 + \hat{f}_2 - f_2) + (\bar{\mathbf{g}}_2 + \hat{\mathbf{g}}_2 - \mathbf{g}_2)u_2 - u_{r2} - d_2 \\ \vdots \\ (\bar{f}_m + \hat{f}_m - f_m) + (\bar{\mathbf{g}}_m + \hat{\mathbf{g}}_m - \mathbf{g}_m)u_m - u_{rm} - d_m \end{bmatrix} \quad (26)$$

We further assume that

$$\begin{aligned} f_i + \mathbf{g}_i u_i &= (\bar{f}_i + \hat{f}_i^*) + (\bar{\mathbf{g}}_i + \hat{\mathbf{g}}_i^*)u_i + \varepsilon_i \\ &= (\bar{f}_i + \Phi_{f_i} \mathbf{w}_{f_i}^*) + (\bar{\mathbf{g}}_i + \Phi_{\mathbf{g}_i} \mathbf{w}_{\mathbf{g}_i}^*)u_i + \varepsilon_i \quad i = 1, 2, \dots, m \end{aligned} \quad (27)$$

$\hat{f}_i^*$  and  $\hat{\mathbf{g}}_i^*$  are the optimal scheme to approximate  $\hat{f}_i$  and  $\hat{\mathbf{g}}_i$ ,  $\mathbf{w}_{f_i}^*$  and  $\mathbf{w}_{\mathbf{g}_i}^*$  are the optimal weight vector. For the mean of  $\Phi_{f_i}$  and  $\Phi_{\mathbf{g}_i}$ , one may refer to equation (17);  $\varepsilon_i$  denotes their difference and is called the approximation error.  $|\varepsilon_i| \leq E_i$ ,  $E_i > 0$ ; we can obtain the following vector notation

$$\mathbf{f} + \mathbf{G}\mathbf{u} = (\bar{\mathbf{f}} + \hat{\mathbf{f}}^*) + (\bar{\mathbf{G}} + \hat{\mathbf{G}}^*)\mathbf{u} + \boldsymbol{\varepsilon}, \quad |\boldsymbol{\varepsilon}| \leq \mathbf{E}. \quad (28)$$

(2) MIMO robust adaptive control design  
Define a Lyapunov function as

$$V = \sum_{i=1}^m V_i, \quad (29)$$

$$V_i = \frac{1}{2} \mathbf{e}_i^T \mathbf{P}_i \mathbf{e}_i + \frac{1}{2\gamma_{f_i}} \tilde{\mathbf{w}}_{f_i}^T \tilde{\mathbf{w}}_{f_i} + \frac{1}{2\gamma_{\mathbf{g}_i}} \tilde{\mathbf{w}}_{\mathbf{g}_i}^T \tilde{\mathbf{w}}_{\mathbf{g}_i} + \frac{1}{2\gamma_{\varepsilon_i}} \tilde{E}_i^2, \quad (30)$$

where  $\tilde{\mathbf{w}}_{f_i} = \mathbf{w}_{f_i} - \mathbf{w}_{f_i}^*$ ,  $\tilde{\mathbf{w}}_{\mathbf{g}_i} = \mathbf{w}_{\mathbf{g}_i} - \mathbf{w}_{\mathbf{g}_i}^*$ , and  $\tilde{E}_i = \hat{E}_i - E_i$ , where  $\hat{E}_i$  is the estimated upper bound, and  $\mathbf{w}_{f_i}^*$ ,  $\mathbf{w}_{\mathbf{g}_i}^*$  are constant optimal weight vectors. The positive definite matrix  $\mathbf{P}_i$  satisfies the following Lyapunov equation:  $\mathbf{A}_i^T \mathbf{P}_i + \mathbf{P}_i \mathbf{A}_i = -\mathbf{Q}_i$ , where  $\mathbf{Q}_i$  is a given positive definite matrix. Taking the derivative of  $V$  with respect to time, we obtain

$$\begin{aligned} \dot{V}_i &= -\frac{1}{2} \mathbf{e}_i^T \mathbf{Q}_i \mathbf{e}_i - \mathbf{e}_i^T \mathbf{P}_i \mathbf{b}_i u_i - \mathbf{e}_i^T \mathbf{P}_i \mathbf{b}_i \varepsilon_i + \frac{1}{\gamma_{\varepsilon_i}} (\hat{E}_i - E_i) \dot{\hat{E}}_i + \\ &\quad \frac{1}{\gamma_{f_i}} (\gamma_{f_i} \mathbf{e}_i^T \mathbf{P}_i \mathbf{b}_i \Phi_{f_i} + \dot{\tilde{\mathbf{w}}}_{f_i}^T) \tilde{\mathbf{w}}_{f_i} + \frac{1}{\gamma_{\mathbf{g}_i}} (\gamma_{\mathbf{g}_i} \mathbf{e}_i^T \mathbf{P}_i \mathbf{b}_i \Phi_{\mathbf{g}_i} u_i + \dot{\tilde{\mathbf{w}}}_{\mathbf{g}_i}^T) \tilde{\mathbf{w}}_{\mathbf{g}_i}. \end{aligned} \quad (31)$$

Furthermore, let  $u_{ri} = \hat{E}_i \cdot \text{sat}_B(\mathbf{e}_i^T \mathbf{P}_i \mathbf{b}_i)$ , where

$$\text{sat}_B(\mathbf{e}_i^T \mathbf{P}_i \mathbf{b}_i) = \begin{cases} \text{sgn}(\mathbf{e}_i^T \mathbf{P}_i \mathbf{b}_i), & |\mathbf{e}_i^T \mathbf{P}_i \mathbf{b}_i| > B \\ \frac{\mathbf{e}_i^T \mathbf{P}_i \mathbf{b}_i}{B}, & \text{otherwise} \end{cases} \quad (32)$$

The adaptive laws are used as the following  $\sigma$ -modification to enhance the robustness of adaptive laws as

$$\dot{\tilde{\mathbf{w}}}_{f_i}^T = -(\gamma_{f_i} \mathbf{e}_i^T \mathbf{P}_i \mathbf{b}_i \Phi_{f_i} + \sigma_{f_i} \mathbf{w}_{f_i}^T), \quad (33)$$

$$\dot{\tilde{\mathbf{w}}}_{\mathbf{g}_i}^T = -(\gamma_{\mathbf{g}_i} \mathbf{e}_i^T \mathbf{P}_i \mathbf{b}_i \Phi_{\mathbf{g}_i} u_i + \sigma_{\mathbf{g}_i} \mathbf{w}_{\mathbf{g}_i}^T), \quad (34)$$

$$\dot{\hat{E}}_i = \gamma_{\varepsilon_i} |\mathbf{e}_i^T \mathbf{P}_i \mathbf{b}_i| - \sigma_{\varepsilon_i} \hat{E}_i, \quad (35)$$

where  $\sigma_{f_i}$ ,  $\sigma_{\mathbf{g}_i}$  and  $\sigma_{\varepsilon_i}$  are the designed parameters.

Accordingly, the definition of (30) yields

$$\begin{aligned} \dot{V}_i &= -\frac{1}{2} \mathbf{e}_i^T \mathbf{Q}_i \mathbf{e}_i - \frac{\sigma_{f_i}}{\gamma_{f_i}} \mathbf{w}_{f_i}^T \tilde{\mathbf{w}}_{f_i} - \frac{\sigma_{\mathbf{g}_i}}{\gamma_{\mathbf{g}_i}} \mathbf{w}_{\mathbf{g}_i}^T \tilde{\mathbf{w}}_{\mathbf{g}_i} + \\ &\quad \frac{1}{\gamma_{\varepsilon_i}} \tilde{E}_i (\gamma_{\varepsilon_i} |\mathbf{e}_i^T \mathbf{P}_i \mathbf{b}_i| - \sigma_{\varepsilon_i} \hat{E}_i) - \mathbf{e}_i^T \mathbf{P}_i \mathbf{b}_i (\hat{E}_i \cdot \text{sat}_B(\mathbf{e}_i^T \mathbf{P}_i \mathbf{b}_i) + \varepsilon_i). \end{aligned} \quad (36)$$

Consider the following case:

$$|\mathbf{e}_i^T \mathbf{P}_i \mathbf{b}_i| \leq B_i, \quad \text{sat}_{B_i}(\mathbf{e}_i^T \mathbf{P}_i \mathbf{b}_i) = \frac{\mathbf{e}_i^T \mathbf{P}_i \mathbf{b}_i}{B_i}. \quad (37)$$

Since

$$\dot{V}_i \leq -\frac{1}{2} \mathbf{e}_i^T \mathbf{Q}_i \mathbf{e}_i - \frac{\sigma_{f_i}}{2\gamma_{f_i}} \tilde{\mathbf{w}}_{f_i}^T \tilde{\mathbf{w}}_{f_i} - \frac{\sigma_{g_i}}{2\gamma_{g_i}} \tilde{\mathbf{w}}_{g_i}^T \tilde{\mathbf{w}}_{g_i} - \frac{3}{4} \frac{\sigma_{e_i}}{2\gamma_{e_i}} \tilde{E}_i^2 + \alpha_i. \quad (38)$$

where

$$\alpha_i \equiv \frac{5}{8} \frac{\sigma_{e_i}}{\gamma_{e_i}} E_i^2 + \frac{1}{4} \frac{\sigma_{e_i}}{\gamma_{e_i}} B_i^2 + \frac{\sigma_{f_i}}{2\gamma_{f_i}} \|\tilde{\mathbf{w}}_{f_i}^*\|^2 + \frac{\sigma_{g_i}}{2\gamma_{g_i}} \|\tilde{\mathbf{w}}_{g_i}^*\|^2, \quad (39)$$

$$\begin{aligned} \dot{V}_i \leq & -\beta_i V + \beta_i V - \frac{1}{2} \mathbf{e}_i^T \mathbf{Q}_i \mathbf{e}_i - \frac{\sigma_{f_i}}{2\gamma_{f_i}} \tilde{\mathbf{w}}_{f_i}^T \tilde{\mathbf{w}}_{f_i} - \frac{\sigma_{g_i}}{2\gamma_{g_i}} \tilde{\mathbf{w}}_{g_i}^T \tilde{\mathbf{w}}_{g_i} - \\ & \frac{3}{4} \frac{\sigma_{e_i}}{2\gamma_{e_i}} \tilde{E}_i^2 + \alpha_i. \end{aligned} \quad (40)$$

Note that  $\lambda_{\min}(\mathbf{Q}_i) \|\mathbf{e}_i\|^2 \leq \mathbf{e}_i^T \mathbf{Q}_i \mathbf{e}_i \leq \lambda_{\max}(\mathbf{Q}_i) \|\mathbf{e}_i\|^2$  and  $\lambda_{\min}(\mathbf{P}_i) \|\mathbf{e}_i\|^2 \leq \mathbf{e}_i^T \mathbf{P}_i \mathbf{e}_i \leq \lambda_{\max}(\mathbf{P}_i) \|\mathbf{e}_i\|^2$ .

We have

$$\begin{aligned} \dot{V}_i \leq & -\beta_i V - [\lambda_{\min}(\mathbf{Q}_i) - \beta_i \lambda_{\max}(\mathbf{P}_i)] \frac{\|\mathbf{e}_i\|^2}{2} - (\sigma_{f_i} - \beta_i) \frac{\tilde{\mathbf{w}}_{f_i}^T \tilde{\mathbf{w}}_{f_i}}{2\gamma_{f_i}} - \\ & (\sigma_{g_i} - \beta_i) \frac{\tilde{\mathbf{w}}_{g_i}^T \tilde{\mathbf{w}}_{g_i}}{2\gamma_{g_i}} + \left(\frac{3}{4} \sigma_{e_i} - \beta_i\right) \frac{\tilde{E}_i^2}{2\gamma_{e_i}} + \alpha_i \end{aligned} \quad (41)$$

We select

$$\beta_i = \min \left\{ \frac{\lambda_{\min}(\mathbf{Q}_i)}{\lambda_{\max}(\mathbf{P}_i)}, \sigma_{f_i}, \sigma_{g_i}, \frac{3}{4} \sigma_{e_i} \right\}, \quad (42)$$

Then

$$\dot{V}_i \leq -\beta_i V + \alpha_i. \quad (43)$$

Obviously, the errors  $\mathbf{e}_i, \tilde{\mathbf{w}}_{f_i}, \tilde{\mathbf{w}}_{g_i}$ , and  $\tilde{E}_i$  are bounded according to Ioannou and Kokotovic [28].

Moreover, if the parameters  $\sigma_{f_i}, \sigma_{g_i}, \frac{3}{4} \sigma_{e_i}$  are selected such that

$$\sigma_{f_i}, \sigma_{g_i}, \frac{3}{4} \sigma_{e_i} \leq \frac{\lambda_{\min}(\mathbf{Q}_i)}{\lambda_{\max}(\mathbf{P}_i)}. \quad (44)$$

We have

$$\dot{V} \leq -\beta_i V - [\lambda_{\min}(\mathbf{Q}_i) - \beta_i \lambda_{\max}(\mathbf{P}_i)] \frac{\|\mathbf{e}_i\|^2}{2} + \alpha_i, \quad (45)$$

if  $[\lambda_{\min}(\mathbf{Q}_i) - \beta_i \lambda_{\max}(\mathbf{P}_i)] \frac{\|\mathbf{e}_i\|^2}{2} - \alpha_i \geq 0$ , then

$$\dot{V}_i \leq -\beta_i V. \quad (46)$$

Thus, the error  $\mathbf{e}_i$  exponentially converges to a set following [29].

$$\|\mathbf{e}_i\|^2 \geq \frac{2\alpha_i}{\lambda_{\min}(\mathbf{Q}_i) - \beta_i \lambda_{\max}(\mathbf{P}_i)}. \quad (47)$$

Smaller  $\sigma_{f_i}, \sigma_{g_i}, \sigma_{e_i}, \beta_i$  can be selected to decrease the residual set of the tracking error. There is always chattering in these systems because of the signum function of compensated controller  $u_{ri} = \hat{E} \cdot \text{sgn}(\mathbf{e}_i^T \mathbf{P}_i \mathbf{b}_i)$ . Clearly, this effect is not desired in practical realization. To overcome this drawback, we should smooth the control signal  $u_{ri}$  to eliminate the unfavorable effects in this paper.

### 4 Simulation Results

Simulations were performed on the trajectory-tracking problem of the mobile robot, as shown in Figure 1. The parameter specifications of the physical model are given as  $a=0.3$  m,  $\rho_r=0.5$  m,  $l=1.75$  m,  $\bar{b}=1.5$  m,  $m_p=20$  kg,  $m'_p=6$  kg,  $m_w=1$  kg,  $m'_w=2$  kg,  $b=1.0$  m,  $\rho_f=0.75$  m, and  $\mu_b = b/a$ .

To illustrate the effectiveness of the proposed B-spline tracking control structure, we use a cubic B-spline function to represent a trajectory and pass through the following intermediate points:

$$\{(-25,0), (-15,5), (-5,2.5), (5,-2.5), (15,-5), (25,0), (15,5), (5,2.5), (-5,-2.5), (-15,-5), (-25,0)\}.$$

The orientation angles of the initial node and final node are  $\tan\theta_s = 8/4$  and  $\tan\theta_g = 8/-4$ , respectively, and the curvature restrictions are set as  $\kappa_j \leq \sqrt{3}$ .

Substituting the above specification into the B-spline optimization algorithm, the resulting trajectory and curvature are shown in Figure 7 and Figure 8, respectively.

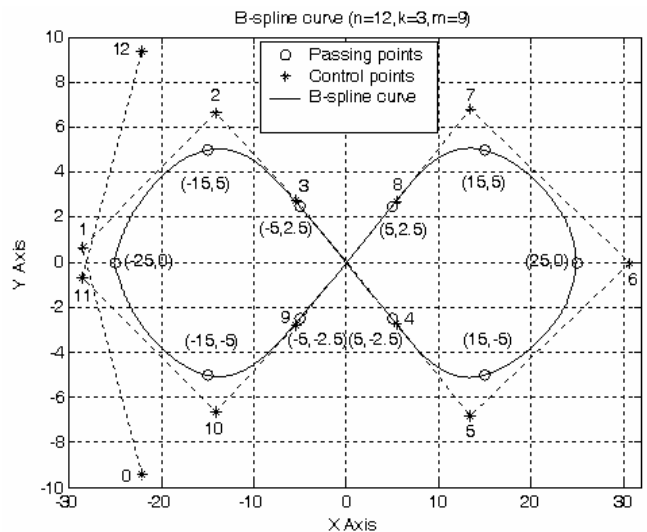
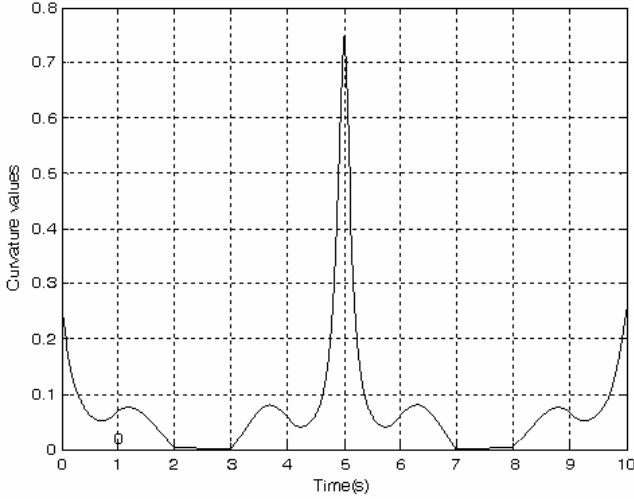


Figure 7. B-spline reference curve



**Figure 8.** Curvature of the B-spline curve

The dynamics of the three-wheeled mobile robot is derived from the reduced Appell equations [26] as follows

$$\begin{aligned} & (m_p(\rho_r^2 + b^2) + I_p + 4m_w b^2 + 2I_w + 8\mu_b^2 I_w) \ddot{\theta} + \\ & (m_p + 2m_w + 2m'_w) ab \ddot{\phi}_1 + m_p a \rho_r \dot{\theta} \dot{\phi}_1 = 2\mu_b \tau_2 \\ & (m_p + 2m_w + 2m'_w) ab \ddot{\theta} + (m_p a^2 + 2m_w a^2 + 4I_w) \ddot{\phi}_1 - \\ & m_p a \rho_r \dot{\theta}^2 = \tau_1 + \tau_2 \end{aligned} \quad (48)$$

Define

$$\begin{aligned} I_w &= \frac{1}{2} m'_w a^2, \\ I_1 &= m_p(\rho_r^2 + b^2) + I_p + 4m_w b^2 + 2I_w + 8\mu_b^2 I_w, \\ I_2 &= m_p a^2 + 2m_w a^2 + 4I_w. \end{aligned} \quad (49)$$

Then, we have

$$I_1 \ddot{\theta} + \mu_b I_2 \ddot{\phi}_1 + m_p a \rho_r \dot{\theta} \dot{\phi}_1 = 2\mu_b \tau_2, \quad (50)$$

$$\mu_b I_2 \ddot{\theta} + I_2 \ddot{\phi}_1 - m_p a \rho_r \dot{\theta}^2 = \tau_1 + \tau_2. \quad (51)$$

Therefore, the dynamical equation of the wheeled mobile robot in the matrix form is

$$\mathbf{M}(\mathbf{y}) \ddot{\mathbf{y}} + \mathbf{C}(\mathbf{y}, \dot{\mathbf{y}}) \dot{\mathbf{y}} = \mathbf{B}(\mathbf{y}) \boldsymbol{\tau}, \quad (52)$$

where

$$\begin{aligned} \mathbf{M}(\mathbf{y}) &= \begin{bmatrix} \mu_b I_2 & I_1 \\ I_2 & \mu_b I_2 \end{bmatrix}, \\ \mathbf{C}(\mathbf{y}, \dot{\mathbf{y}}) &= \begin{bmatrix} m_p a \rho_r \dot{\theta} & 0 \\ 0 & -m_p a \rho_r \dot{\theta} \end{bmatrix}, \\ \mathbf{B}(\mathbf{y}) &= \begin{bmatrix} 0 & 2\mu_b \\ 1 & 1 \end{bmatrix}, \quad \mathbf{y} = \begin{bmatrix} \phi_1 \\ \theta \end{bmatrix}. \end{aligned} \quad (53)$$

After some manipulations, a different type of dynamical equation (20) may be shown in the following form

$$\mathbf{f}(\mathbf{x}) = \begin{bmatrix} x_2 \\ \frac{\mu_b}{I_1 - \mu_b^2 I_2} (m_p a \rho_r x_4 x_2) + \frac{I_1 / I_2}{I_1 - \mu_b^2 I_2} (m_p a \rho_r x_4^2) \\ x_4 \\ -\frac{1}{I_1 - \mu_b^2 I_2} (m_p a \rho_r x_4 x_2) - \frac{\mu_b}{I_1 - \mu_b^2 I_2} (m_p a \rho_r x_4^2) \end{bmatrix}, \quad (54)$$

$$\mathbf{G}(\mathbf{x}) = \begin{bmatrix} 0 & 0 \\ \frac{I_1 / I_2}{I_1 - \mu_b^2 I_2} & \frac{-2\mu_b^2}{I_1 - \mu_b^2 I_2} + \frac{I_1 / I_2}{I_1 - \mu_b^2 I_2} \\ 0 & 0 \\ \frac{-\mu_b}{I_1 - \mu_b^2 I_2} & \frac{\mu_b}{I_1 - \mu_b^2 I_2} \end{bmatrix}, \quad (55)$$

where  $\mathbf{x} = [x_1 \ x_2 \ x_3 \ x_4]^T = [\phi_1 \ \dot{\phi}_1 \ \theta \ \dot{\theta}]^T$ .

Next, the desired values of other system variables  $(\varphi_d(t), \theta_d(t))$  are computed according to Tsai [26]. Based on the current status of the vehicle and the fuzzy inference engine in Subsection 3.1, the compensations  $\mathbf{u}_c$  and  $\mathbf{y}_c$  are computed from the fuzzy logic system and fed into the FCMAC controller as described in Subsection 3.2. In the adaptive scheme, the initial condition is used, which is different from the true value. Moreover, we set the initial posture as  $x_r(0) = -7.5$ ,  $y_r(0) = 0$ , and  $x_r(0) = -17.5$ ,  $y_r(0) = 0$  away from the desired values  $(-12.5, 0)$ . The parameters of the Gaussian functions of FCMAC are constructed on each layer in equation (16), where  $s_1 = [-4, 4]$ ,  $s_2 = [-4, 4]$ .

The means and variances are

$$\sigma_{mj} = \sigma_{mk} = 1 \quad (m = 1, 2, 3, j = 1, 2, k = 1, 2)$$

and

$$\begin{aligned} m_{nj} = m_{nk} &= -1 \quad (m = 1, j = k = 1), m_{nj} = m_{nk} = 5 \quad (m = 1, j = k = 2) \\ m_{nj} = m_{nk} &= -5 \quad (m = 2, j = k = 1), m_{nj} = m_{nk} = 1 \quad (m = 2, j = k = 2) \\ m_{nj} = m_{nk} &= -3 \quad (m = 3, j = k = 1), m_{nj} = m_{nk} = 3 \quad (m = 3, j = k = 2) \end{aligned} \quad (56)$$

The parameters of the control scheme in equation (24) are:

$$\boldsymbol{\Lambda} = \left[ \begin{array}{cc|cc} 200 & 30 & 0 & 0 \\ 0 & 0 & 200 & 30 \end{array} \right]. \quad (57)$$

The parameters of the adaptive laws in equations (33) and (34) are:

$$\gamma_{f_1} = 60, \gamma_{f_2} = 40, \gamma_{g_1} = 4, \gamma_{g_2} = 2, \sigma_{f_1} = \sigma_{f_2} = 0.4, \sigma_{g_1} = \sigma_{g_2} = 0.1,$$

$$\mathbf{Q} = \left[ \begin{array}{cc|cc} 30 & 0 & 0 & 0 \\ 0 & 30 & 0 & 0 \\ \hline 0 & 0 & 30 & 0 \\ 0 & 0 & 0 & 30 \end{array} \right], \quad (58)$$

which yields the corresponding **A** and **P** as follows

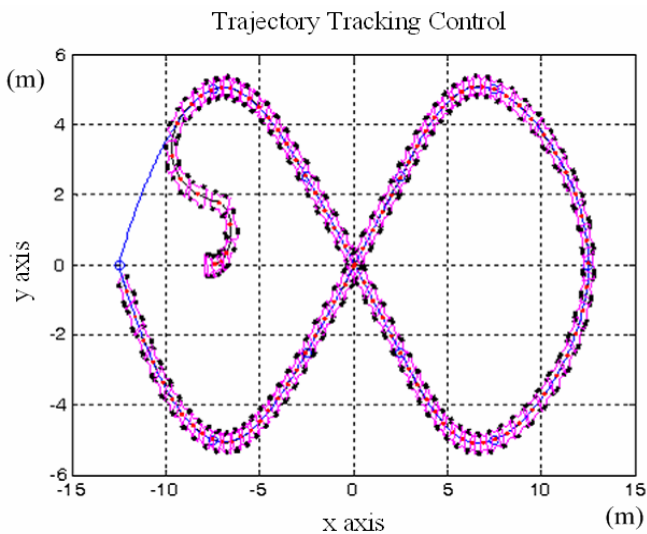
$$\mathbf{A} = \left[ \begin{array}{cc|cc} \mathbf{A}_1 & \mathbf{0} & & \\ \mathbf{0} & \mathbf{A}_2 & & \end{array} \right] = \left[ \begin{array}{cc|cc} 0 & 1 & 0 & 0 \\ -200 & -30 & 0 & 0 \\ \hline 0 & 0 & 0 & 1 \\ 0 & 0 & -200 & -30 \end{array} \right],$$

$$\mathbf{P} = \left[ \begin{array}{cc|cc} 102.75 & 0.075 & 0 & 0 \\ 0.075 & 0.5025 & 0 & 0 \\ \hline 0 & 0 & 102.75 & 0.075 \\ 0 & 0 & 0.075 & 0.5025 \end{array} \right] \quad (59)$$

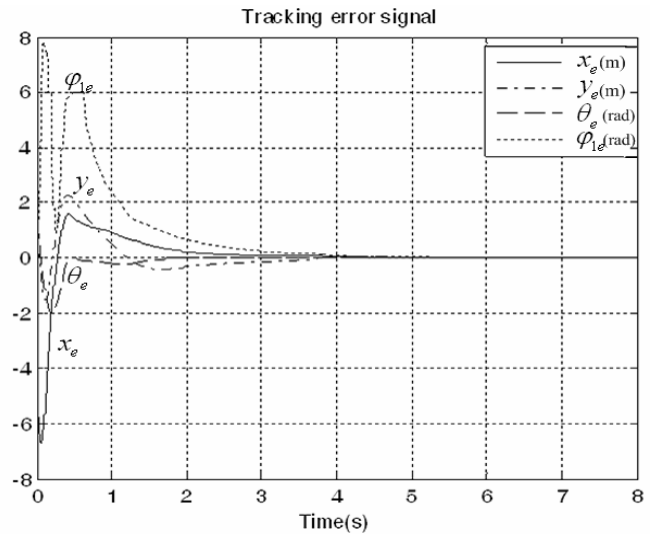
The parameters of the robust terms in equation (35) are

$$\gamma_{e_1} = 0.01, \gamma_{e_2} = 0.1, \sigma_{e_1} = 0.01, \sigma_{e_2} = 0.1 \quad (60)$$

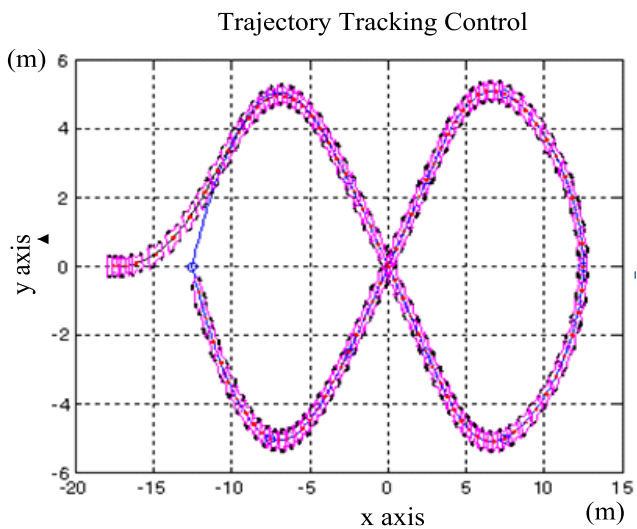
The results are shown in Figure 9. The solid line is the desired B-spline curve, and the shaded block line shows the tracking performance. Although the initial condition is significantly far from the desired configuration in both position and heading, the proposed hierarchical controller can successfully steer the mobile robot back to the desired trajectory.



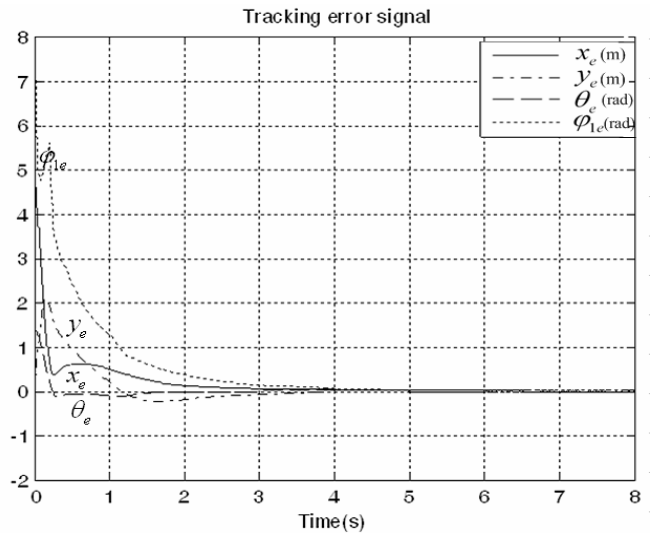
(a) The trajectory tracking for the initial posture:  $x_r(0) = -7.5, y_r(0) = 0$



(b) The tracking error signals for the initial posture:  $x_r(0) = -7.5, y_r(0) = 0$



(c) The trajectory tracking for the initial posture:  $x_r(0) = -17.5, y_r(0) = 0$



(d) The tracking error signals for the initial posture:  $x_r(0) = -17.5, y_r(0) = 0$

**Figure 9.** The trajectory tracking performance in different initial posture

## 5 Conclusions

A new systematic design procedure to track the trajectory of mobile robots is developed in this paper. The main results are summarized as follows:

(1) The concept of the methodology is a combined application of the path-planning techniques and trajectory-tracking control. The constrained optimization method can be used to determine a unique set of control points so that the cubic B-spline curve can pass through the given intermediate points with uniform knots, which are subject to the kinematic constraints and curvature restrictions.

(2) Because of the local tuning property of the B-spline curve, the sharp modification of the trajectory is notably flexible and effective.

(3) The adaptive tracking controller is constructed for the hierarchical model based on the fuzzy inference methodology. The main advantage of the proposed fuzzy controller is its capability to provide a desired reference in designing the adaptive FCMAC control in the dynamic model of the mobile robot.

(4) The design of the adaptive FCMAC controller based on the stability analysis is used to address the parametric uncertainties and guarantee the stabilization of the motion to a desired configuration.

The simulation results show that the proposed B-spline trajectory tracking strategy achieves the desired tracking performance.

## Acknowledgments

The authors would like to thank the Ministry of Science and Technology, Taiwan, R.O.C., for financially supporting this study under Contract No. MOST 106-2622-E-197-010-CC3.

## References

- [1] C. de Boor, *A Practical Guide to Splines*, Springer-Verlag, 1978.
- [2] M. G. Cox, The Numerical Evaluation of B-Splines, *IMA Journal of Applied Mathematics*, Vol. 10, No. 2, pp. 134-149, October, 1972.
- [3] S. Okaniwa, A. Nasri, H. Lin, A. Abbas, Y. Kineri, T. Maekawa, Uniform B-Spline Curve Interpolation with Prescribed Tangent and Curvature Vectors, *IEEE Transactions on Visualization and Computer Graphics*, Vol. 18, No. 9, pp. 1474-1487, September, 2012.
- [4] L. Zhang, X. Ge, J. Tan, Least Square Geometric Iterative Fitting Method for Generalized B-Spline Curves with Two Different Kinds of Weights, *The Visual Computer*, Vol. 32, No. 9, pp. 1109-1120, September, 2016.
- [5] W. J. Gordon, R. F. Riesenfeld, B-Spline Curves and Surfaces, in: R. Bamhill, R. F. Riesenfeld (Eds.), *Computer Aided Geometric Design*, Academic Press, New York, 1974, pp. 95-126.
- [6] A. N. Ravari, H. D. Taghirad, Reconstruction of B-Spline Curves and Surfaces by Adaptive Group Testing, *Computer Aided Geometric Design*, Vol. 74, pp. 32-44, May, 2016.
- [7] H. C. Huang, An Evolutionary Optimal Fuzzy System With Information Fusion of Heterogeneous Distributed Computing and Polar-Space Dynamic Model for Online Motion Control of Swedish Redundant Robots, *IEEE Transactions on Industrial Electronics*, Vol. 64, No. 2, pp. 1743-1750, February, 2017.
- [8] H. C. Huang, C. H. Chiang, An Evolutionary Radial Basis Function Neural Network with Robust Genetic-Based Immune computing for Online Tracking Control of Autonomous Robots, *Neural Processing Letters*, Vol. 44, No. 1, pp. 19-35, August, 2016.
- [9] R. F. Riesenfeld, *Applications of B-spline Approximation to Geometric Problems of Computer Aided Design*, Ph.D. Dissertation, Syracuse University, Syracuse, NY, 1972.
- [10] C. C. Yih, Time-Varying Control for Exponential Stabilisation of the Brockett Integrator, *IET Control Theory & Applications*, Vol. 11, No. 12, pp. 1976-1982, July, 2017.
- [11] R. W. Brockett, *Asymptotic Stability and Feedback Stabilization*, in: R. W. Brockett, R. S. Millman, H. J. Sussmann (Eds.), *Differential Geometric Control Theory*, Birkhauser, 1983, pp. 181-191.
- [12] J. Guldner, V. I. Utkin, Sliding Mode Control for Gradient Tracking and Robot Navigation Using Artificial Potential Fields, *IEEE Transactions on Robotics and Automation*, Vol. 11, No. 2, pp. 247-254, April, 1995.
- [13] R. M. Murray, S. S. Sastry, Nonholonomic Motion Planning: Steering Using Sinusoids, *IEEE Transactions on Automatic Control*, Vol. 38, No. 5, pp. 700-716, May, 1993.
- [14] C. Samson, Control of Chained System: Application to Path Following and Time-Varying Point-Stabilization of Mobile Robots, *IEEE Transactions on Automatic Control*, Vol. 40, No. 1, pp. 64-77, January, 1995.
- [15] D. Chwa, Sliding-Mode Tracking Control of Nonholonomic Wheeled Mobile Robots in Polar Coordinates, *IEEE Transactions on Control Systems Technology*, Vol. 12, No. 4, pp. 637-644, July, 2004.
- [16] S. Sun, Designing Approach on Trajectory- Tracking Control of Mobile Robot, *Robotics and Computer-Integrated Manufacturing*, Vol. 21, No. 1, pp. 81-85, February, 2005.
- [17] R. Fierro, F. L. Lewis, Control of a Nonholonomic Mobile: Backstepping Kinematics into Dynamics, *Proceedings of the 34th IEEE Conference on Decision and Control*, New Orleans, LA, 1995, pp. 3805-3810.
- [18] S. S. Ge, G. Y. Zhou, Adaptive Robust Stabilization of Dynamic Nonholonomic Chained Systems, *Journal of Field Robotics*, Vol. 18, No. 3, pp. 119-133, February, 2001.
- [19] W. Dong, W. Huo, Adaptive Stabilization of Uncertain Dynamic Non-holonomic Systems, *International Journal of Control*, Vol. 72, No. 18, pp. 1689-1700, 1999.
- [20] T. Das, I. N. Kar, S. Chaudhury, Simple Neuron-Based Adaptive Controller for a Nonholonomic Mobile Robot

- Including Actuator Dynamics, *Neurocomputing*, Vol. 69, No. 16-18, pp. 2140-2151, October, 2006.
- [21] K. Rajeswari, S. Neduncheliyan, Genetic Algorithm Based Fault Tolerant Clustering in Wireless Sensor Network, *IET Communications*, Vol. 11, No. 12, pp. 1927-1932, August, 2017.
- [22] D. Das, S. Das, Adaptive Resource Allocation Scheme for Cognitive Radio Vehicular Ad-Hoc Network in the Presence of Primary User Emulation Attack, *IET Networks*, Vol. 6, No. 1, pp. 5-13, January, 2017.
- [23] B. Shen, N. W. Wang, H. H. Qiu, A New Genetic Algorithm for Overlapping Community Detection, *Journal of Internet Technology*, Vol. 15, No. 7, pp. 1143-1150, December, 2014.
- [24] H. Wu, M. Zhao, Genetic Algorithm with Fuzzy Inference for Convergence Acceleration, *Journal of Internet Technology*, Vol. 18, No. 4, pp. 919-926, July, 2017.
- [25] H. Ma, Y. C. Tseng, L. I. Chen, A CMAC-based Scheme for Determining Membership with Classification of Text Strings, *Neural Computing and Applications*, Vol. 27, pp. 1959-1967, 2016.
- [26] P. S. Tsai, *Modeling and Control for Wheeled Mobile Robots with Nonholonomic Constraints*, Ph.D. Dissertation, National Taiwan University, Taipei, Taiwan, 2006.
- [27] J. Y. Chen, P. S. Tsai, C. C. Wong, Adaptive Design of a Fuzzy Cerebellar Model Arithmetic Controller Neural Network, *IEE Proceedings-Control Theory and Applications*, Vol. 152, No. 2, pp. 133-137, March, 2005.
- [28] P. A. Ioannou, P. V. Kokotovic, Instability Analysis and Improvement Robustness of Adaptive Control, *Automatica*, Vol. 20, No. 5, pp. 583-594, September, 1984.
- [29] T. F. Wu, P. S. Tsai, F. R. Chang, L. S. Wang, Adaptive Fuzzy CMAC Control for a Class of Nonlinear Systems with Smooth Compensation, *IEE Proceedings-Control Theory and Applications*, Vol. 153, No. 6, pp. 647- 657, November, 2006.

## Biography



**Ter-Feng Wu** was born in Taiwan in 1962. He received the B.S. degree in Department of Industrial Education from National Taiwan Normal University, Taipei, Taiwan, in 1986. He received the M.S. degree in Department of Control Engineering from National Chiao Tung University, Hsinchu, Taiwan, in 1993. He received the Ph.D. degree in Department Electrical Engineering from National Taiwan University, Taipei, Taiwan, in 2006. He is currently an associate professor and was a chair in 2009-2015 at the Department of Electrical Engineering, National Ilan University, Yilan, Taiwan. His research interests include intelligent control, neural network, fuzzy CMAC, mobile robot, multi-rotor UAVs and green energy technology, etc.

## Appendix A

List of Symbols:

- $\{\mathbf{E}^x, \mathbf{E}^y, \mathbf{E}^z\}$ : inertial frame
- $\{\mathbf{e}_j^x, \mathbf{e}_j^y, \mathbf{e}_j^z\}$ : body frame
- $\theta_i, \psi_i, \varphi_i$ : heading angle, camber angle, spin angle of body  $i$
- $x_i, y_i, z_i$ :  $x$ -axis,  $y$ -axis,  $z$ -axis motion of body  $i$
- $C_i$ : mass center of body  $i$ , where  $i=1, 2, p$ .
- $Q_r$ : center of the left wheel and right wheel
- $b$ : distance between the two wheels (wheelbase)
- $\bar{b}, \ell, a$ : width and length of the platform, radius of the wheel
- $m'_w, m'_p$ : masses of the rim of each wheel and platform
- $m_w, m_p$ : masses of each wheel and platform
- $\rho_r$ : distance between point  $Q_r$  and mass center of platform  $C_p$
- $x_r, y_r$ :  $x$ -axis,  $y$ -axis motion in terms of the coordinates of  $Q_r$
- $\mathbf{q}$ : generalized coordinate
- $\mathbf{D}$ : nonholonomic constraint matrix
- $\mathbf{u} = (\dot{\varphi}_1, \dot{\theta})$ : privileged velocity
- $\mathbf{u}_d$ : desired privileged velocity
- $A_i, B_i, C_i, D_i, E_i$ : fuzzy sets for the  $i$ th rule
- $d_e$ : error distance between the current position and the desired position
- $\theta_e$ : error angle between the current and desired heading angles
- $\theta_e'$ : orientation angle from the current position to the desired position
- $\Delta v, \Delta \omega$ : compensated values of the linear velocity and angular velocity
- $\xi_e$ : posture error vector in the body frame
- $F$ : nonlinear mapping of the CMAC
- $\mathbf{S}$ : input variable of the CMAC
- $\mathbf{z}_{CMAC}$ : output variable of the CMAC
- $\phi(s)$ : receptive-field functions
- $m, \sigma$ : mean and variance of the Gaussian function
- $\phi_{mjk}$ : multi-dimensional receptive-field functions
- $n_l, n_b$ : number of layers and number of blocks in each layer
- $\mathbf{w}$ : weight vector of the FCMAC
- $\Phi$ : vector of multi-dimensional receptive-field functions
- $\mathbf{f}$ : system dynamics vector,  $\mathbf{f} = [f_1(\mathbf{x}), f_2(\mathbf{x}), \dots, f_m(\mathbf{x})]^T$
- $\mathbf{G}$ : continuous bounded matrix,  $\mathbf{G}(\mathbf{x}) = [g_1(\mathbf{x}), g_2(\mathbf{x}), \dots, g_n(\mathbf{x})]$
- $\mathbf{d}$ : disturbance,  $\mathbf{d}(\mathbf{x}, t) = [d_1(\mathbf{x}, t), d_2(\mathbf{x}, t), \dots, d_m(\mathbf{x}, t)]^T$
- $\mathbf{u}$ : control input  $\mathbf{u} = [u_1, u_2, \dots, u_m]^T$
- $\mathbf{e}$ : tracking error vector,  $\mathbf{e} = [\mathbf{e}_1^T \quad \mathbf{e}_2^T \quad \dots \quad \mathbf{e}_m^T]^T \in R^n$

$\Lambda$ : designed positive constant matrix

$\tilde{\mathbf{f}}, \tilde{\mathbf{G}}$ : uncertainties of dynamics

$\tilde{f}_i^*, \tilde{\mathbf{g}}_i^*$ : optimal scheme to approximate  $\tilde{f}_i$  and  $\tilde{\mathbf{g}}_i$

$\mathbf{w}_{f_i}^*, \mathbf{w}_{g_i}^*$ : optimal weight vector

$\Phi_{f_i}, \Phi_{g_i}$ : vector of the receptive-field functions associated with  $\tilde{f}_i$  and  $\tilde{\mathbf{g}}_i$

$\varepsilon_i$ : approximation error

$\gamma_{f_1}, \gamma_{f_2}, \gamma_{g_1}$ : parameters of the adaptive laws

$\gamma_{g_2}, \gamma_{e_1}, \gamma_{e_2}$

$\mathbf{P}_i, \mathbf{Q}_i$ : positive definite matrices, which satisfy the following Lyapunov equation:  $\mathbf{A}_i^T \mathbf{P}_i + \mathbf{P}_i \mathbf{A}_i = -\mathbf{Q}_i$ .

## Appendix B

### Kinematic Level

$$\mathbf{u}_c = \mathbf{u}_d + \Delta \mathbf{u}, \quad \begin{bmatrix} v_c \\ w_c \end{bmatrix} = \begin{bmatrix} v_d \\ w_d \end{bmatrix} + \begin{bmatrix} \Delta v \\ \Delta w \end{bmatrix}. \quad (61)$$

Using a fuzzy inference engine to design  $\Delta \mathbf{u}$  in the kinematic level, and  $\mathbf{u}_d$  is desired signal from motion planning.

Dynamic Level (Eq. 62)

$$\mathbf{y}^{(r)} = \mathbf{f}(\mathbf{x}) + \mathbf{G}(\mathbf{x})\mathbf{u}, \quad (62)$$

where  $\mathbf{x} = [x_1 \ x_2 \ x_3 \ x_4]^T = [\varphi_1 \ \dot{\varphi}_1 \ \theta \ \dot{\theta}]^T$ . Our purpose is to design the control input in dynamic level

$$\mathbf{u} = (\bar{\mathbf{G}} + \hat{\mathbf{G}})^{-1} [-\bar{\mathbf{f}} - \hat{\mathbf{f}} + \mathbf{y}_d^{(r)} + \Lambda^T \mathbf{e} + \mathbf{u}_r], \quad (63)$$

such that dynamic output signal  $\mathbf{x} = [x_1 \ x_2 \ x_3 \ x_4]^T$  approximate to the kinematic  $\mathbf{u}_c$ , i.e.  $\dot{\varphi}_1 \rightarrow v_c$  and  $\dot{\theta} \rightarrow w_c$ .

[Case I] Consider the following Multi-Input Multi-Output (MIMO) system:

$$\mathbf{y}^{(r)} = \mathbf{f}(\mathbf{x}) + \mathbf{G}(\mathbf{x})\mathbf{u}, \quad (64)$$

if the system dynamics  $\mathbf{f}(\mathbf{x})$ ,  $\mathbf{G}(\mathbf{x})$  are known, where

$$\mathbf{f}(\mathbf{x}) = \begin{bmatrix} x_2 \\ \frac{\mu_b}{I_1 - \mu_b^2 I_2} (m_p a \rho_r x_4 x_2) + \frac{I_1 / I_2}{I_1 - \mu_b^2 I_2} (m_p a \rho_r x_4^2) \\ x_4 \\ -\frac{1}{I_1 - \mu_b^2 I_2} (m_p a \rho_r x_4 x_2) - \frac{\mu_b}{I_1 - \mu_b^2 I_2} (m_p a \rho_r x_4^2) \end{bmatrix} \quad (65)$$

$$\mathbf{G}(\mathbf{x}) = \begin{bmatrix} 0 & 0 \\ \frac{I_1 / I_2}{I_1 - \mu_b^2 I_2} & \frac{-2\mu_b^2}{I_1 - \mu_b^2 I_2} + \frac{I_1 / I_2}{I_1 - \mu_b^2 I_2} \\ 0 & 0 \\ \frac{-\mu_b}{I_1 - \mu_b^2 I_2} & \frac{\mu_b}{I_1 - \mu_b^2 I_2} \end{bmatrix} \quad (66)$$

Controller design in dynamics is  $\mathbf{u} = (\mathbf{G})^{-1} [-\mathbf{f} + \mathbf{y}_d^{(r)} + \Lambda^T \mathbf{e}]$ , and simulation results as following.

The blue and red are the desired B-spline curve of left and right wheels of 3-wheel mobile robot in Figure 10, and the shaded block line shows the tracking performance in Figure 11.

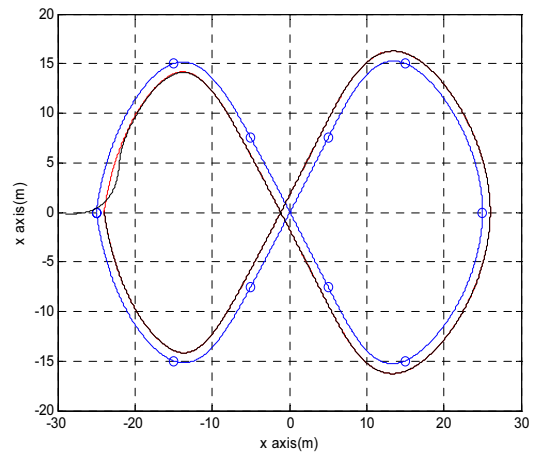


Figure 10. The desired B-spline curve of left and right wheels of 3-wheel mobile robot

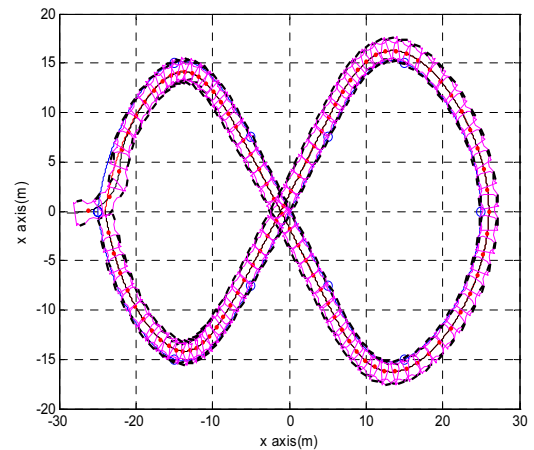


Figure 11. The tracking performance

The trajectory tracking effect of privileged variable shown in Figure 12, where  $[v_c \ w_c]^T$  is designed by fuzzy inference engine in kinematics, and  $[\dot{\varphi}_1 \ \dot{\theta}]^T$  is designed by FCMAC in dynamics. Tracking errors of generalized variables show in Figure 13, where

$$x_e = x_{rd} - x_r, \ y_e = y_{rd} - y_r, \ \theta_e = \theta_d - \theta, \ \varphi_{1e} = \varphi_{1d} - \varphi_1. \quad (67)$$

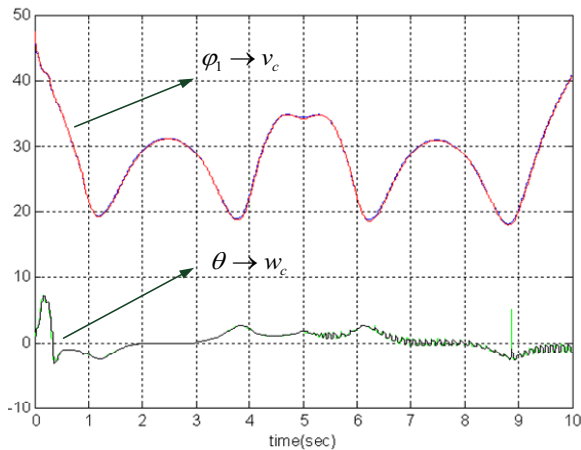


Figure 12. The trajectory tracking effect of privileged variable

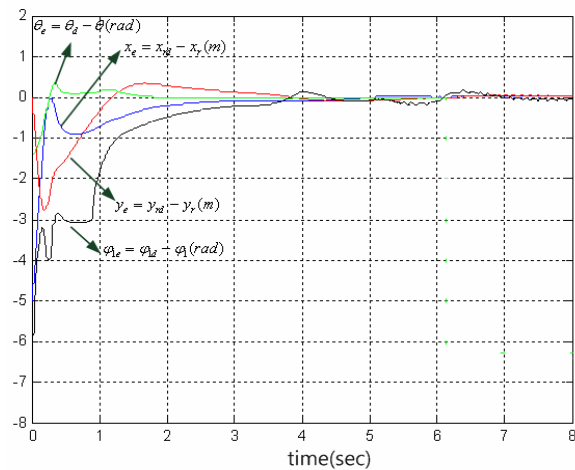


Figure 13. Tracking errors of generalized variables

[Case II] Consider the following Multi-Input Multi-Output (MIMO) system:

$$y^{(r)} = (\bar{f}(x) + \hat{f}(x)) + G(x)u, \tag{68}$$

$f(x)$  exists parametric uncertainties, where  $\hat{f}$  is uncertain part and  $\bar{f}$  is nominal models.

$$f(x) = \begin{bmatrix} x_2 \\ \frac{\mu_b}{I_1 - \mu_b^2 I_2} (m_p a \rho_r x_4 x_2) + \frac{I_1 / I_2}{I_1 - \mu_b^2 I_2} (m_p a \rho_r x_4^2) + \Delta f_1 \\ x_4 \\ \frac{1}{I_1 - \mu_b^2 I_2} (m_p a \rho_r x_4 x_2) - \frac{\mu_b}{I_1 - \mu_b^2 I_2} (m_p a \rho_r x_4^2) + \Delta f_2 \end{bmatrix}, \tag{69}$$

$\Delta f_1 = 20, \Delta f_2 = 20.$

$$G(x) = \begin{bmatrix} 0 & 0 \\ \frac{I_1 / I_2}{I_1 - \mu_b^2 I_2} & \frac{-2\mu_b^2}{I_1 - \mu_b^2 I_2} + \frac{I_1 / I_2}{I_1 - \mu_b^2 I_2} \\ 0 & 0 \\ \frac{-\mu_b}{I_1 - \mu_b^2 I_2} & \frac{\mu_b}{I_1 - \mu_b^2 I_2} \end{bmatrix} \tag{70}$$

Adopting the controller in dynamics as

$$u = (G)^{-1} [-f + y_d^{(r)} + \Lambda^T e]. \tag{71}$$

Obviously, simulation result in Figure 14 can not achieve the desired effects.

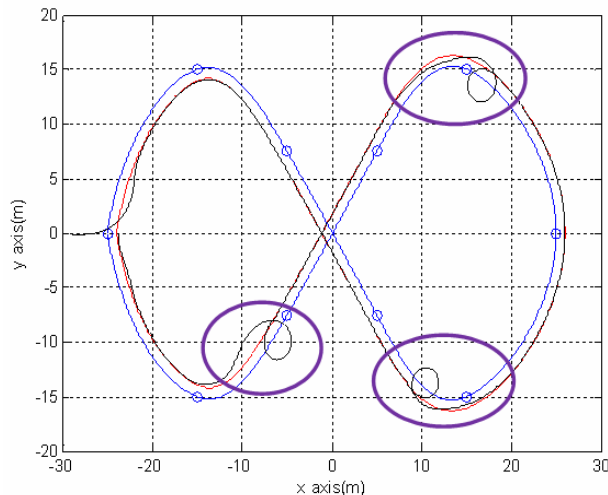


Figure 14. The tracking performance of the controller in dynamics

[Case III] Follow the previous example, using the FCMAC controller

$$u = (G)^{-1} [-\bar{f} - \hat{f} + y_d^{(r)} + \Lambda^T e] \tag{72}$$

$$\hat{f} = \hat{f}(x|w)$$

$$\hat{f}_i = \Phi_{f_i} w_{f_i}, \dot{w}_{f_i}^T = -\gamma_{f_i} e_i^T P b_i \Phi_{f_i}, i=1,2$$

The trajectory tracking performance is shown in Figure 15. Figure 16 illustrate the trajectory tracking effect of privileged variable and tracking error of generalized variables show in Figure 17.

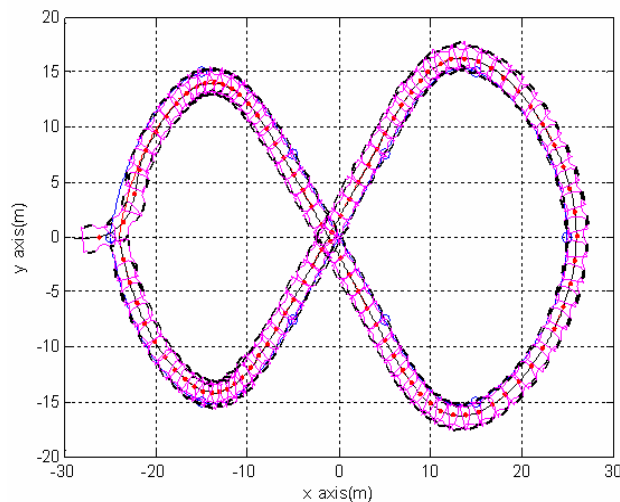
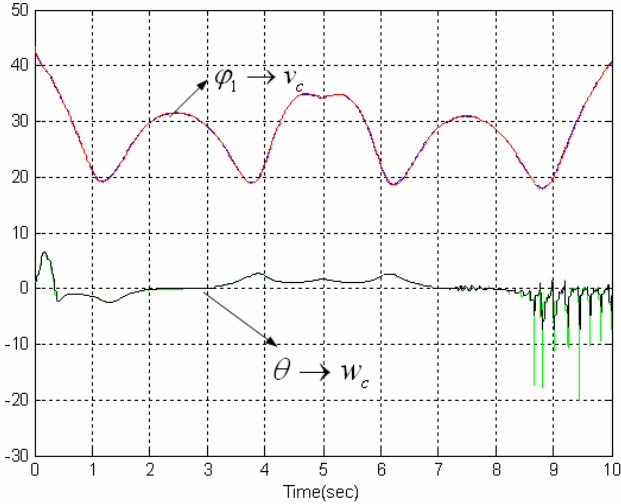
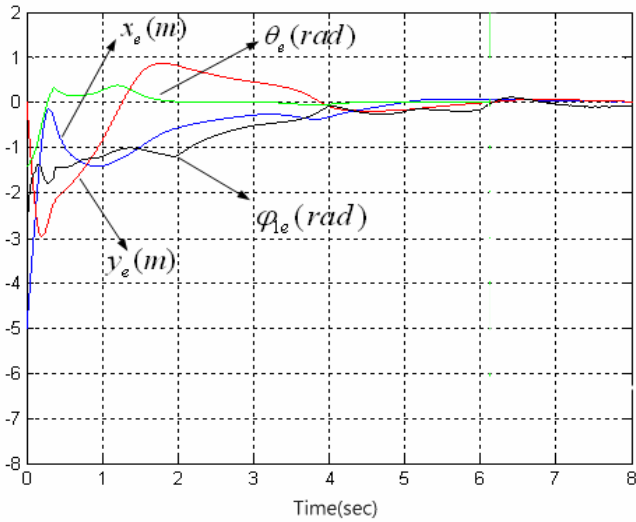


Figure 15. The trajectory tracking performance



**Figure 16.** The trajectory tracking effect of privileged variable



**Figure 17.** Tracking error of generalized variables

**[Case IV]** Consider the following Multi-Input Multi-Output (MIMO) system with disturbance  $\mathbf{d}(t)$ :

$$\mathbf{y}^{(r)} = (\bar{\mathbf{f}}(\mathbf{x}) + \hat{\mathbf{f}}(\mathbf{x})) + \mathbf{G}(\mathbf{x})\mathbf{u} + \mathbf{d}(t), \quad (73)$$

$\hat{\mathbf{f}}(\mathbf{x})$  exists parametric uncertainties, where  $\hat{\mathbf{f}}$  is uncertain part and  $\bar{\mathbf{f}}$  is nominal models.

$$\mathbf{f}(\mathbf{x}) = \begin{bmatrix} x_2 \\ \frac{\mu_b}{I_1 - \mu_b^2 I_2} (m_p a \rho_r x_4 x_2) + \frac{I_1 / I_2}{I_1 - \mu_b^2 I_2} (m_p a \rho_r x_4^2) + \Delta f_1 \\ x_4 \\ -\frac{1}{I_1 - \mu_b^2 I_2} (m_p a \rho_r x_4 x_2) - \frac{\mu_b}{I_1 - \mu_b^2 I_2} (m_p a \rho_r x_4^2) + \Delta f_2 \end{bmatrix}, \quad (74)$$

$\Delta f_1 = 20, \Delta f_2 = 20.$

$\mathbf{d}(t) = (10 * rand)$ , rand denotes random number,  $0 < rand < 1$ .

$$\mathbf{G}(\mathbf{x}) = \begin{bmatrix} 0 & 0 \\ \frac{I_1 / I_2}{I_1 - \mu_b^2 I_2} & \frac{-2\mu_b^2}{I_1 - \mu_b^2 I_2} + \frac{I_1 / I_2}{I_1 - \mu_b^2 I_2} \\ 0 & 0 \\ \frac{-\mu_b}{I_1 - \mu_b^2 I_2} & \frac{\mu_b}{I_1 - \mu_b^2 I_2} \end{bmatrix} \quad (75)$$

Adopting the controller in dynamics as

$$\mathbf{u} = (\mathbf{G})^{-1} \left[ -\bar{\mathbf{f}} - \hat{\mathbf{f}} + \mathbf{y}_d^{(r)} + \Lambda^T \mathbf{e} \right]$$

$$\hat{\mathbf{f}} = \hat{\mathbf{f}}(\mathbf{x}|\mathbf{w}) \quad (76)$$

$$\hat{f}_i = \Phi_{f_i} \mathbf{w}_{f_i}, \dot{\mathbf{w}}_{f_i}^T = -\gamma_{f_i} \mathbf{e}_i^T \mathbf{P}_i \mathbf{b}_i \Phi_{f_i}, i=1,2$$

Obviously, simulation result in Figure 18 can not achieve the desired effects.

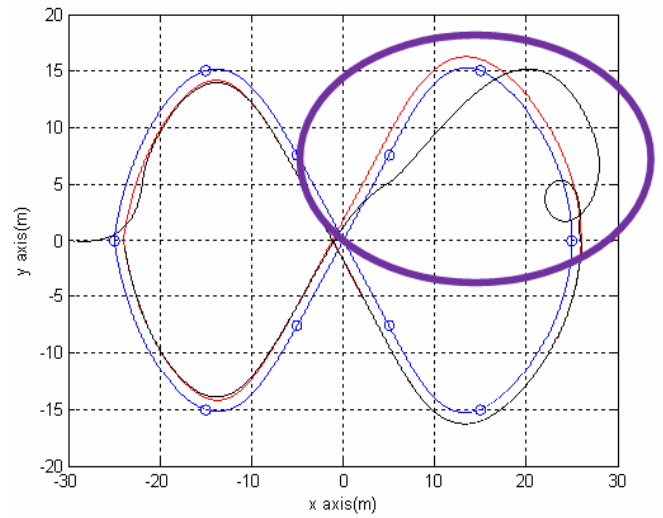


**Figure 18.** The tracking performance of the controller in dynamics

**[Case V]** Follow the previous example, using the FCMAC controller with chattering robust term

$$\mathbf{u} = (\mathbf{G})^{-1} \left[ -\bar{\mathbf{f}} - \hat{\mathbf{f}} + \mathbf{y}_d^{(r)} + \Lambda^T \mathbf{e} + \mathbf{u}_r \right]$$

$$\hat{\mathbf{f}} = \hat{\mathbf{f}}(\mathbf{x}|\mathbf{w})$$

$$\hat{f}_i = \Phi_{f_i} \mathbf{w}_{f_i}, \dot{\mathbf{w}}_{f_i}^T = -\gamma_{f_i} \mathbf{e}_i^T \mathbf{P}_i \mathbf{b}_i \Phi_{f_i}, i=1,2 \quad (77)$$

$$u_{ri} = \hat{E}_i \cdot \text{sgn}(\mathbf{e}_i^T \mathbf{P}_i \mathbf{b}_i), \text{ where } \hat{E}_i = \gamma_{e_i} |\mathbf{e}_i^T \mathbf{P}_i \mathbf{b}_i|$$

$$\text{and } \text{sgn}(e) = \begin{cases} 1, & e > 0 \\ 0, & e = 0 \\ -1, & e < 0 \end{cases}$$

The trajectory tracking performance is shown in Figure 19. Figure 20 illustrate the trajectory tracking effect of privileged variable and tracking error of generalized variables show in Figure 21.

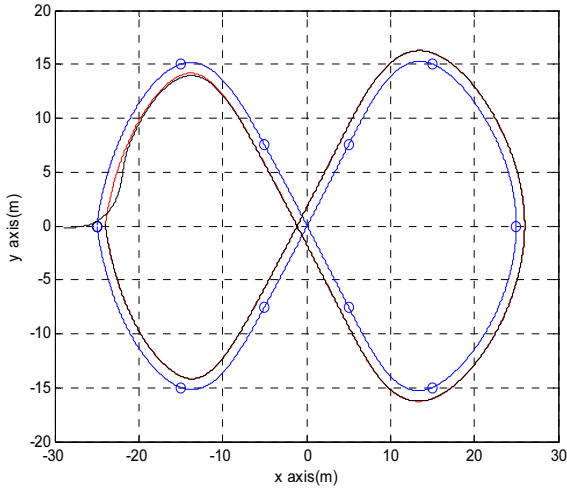


Figure 19. The desired B-spline curve of left and right wheels of 3-wheel mobile robot

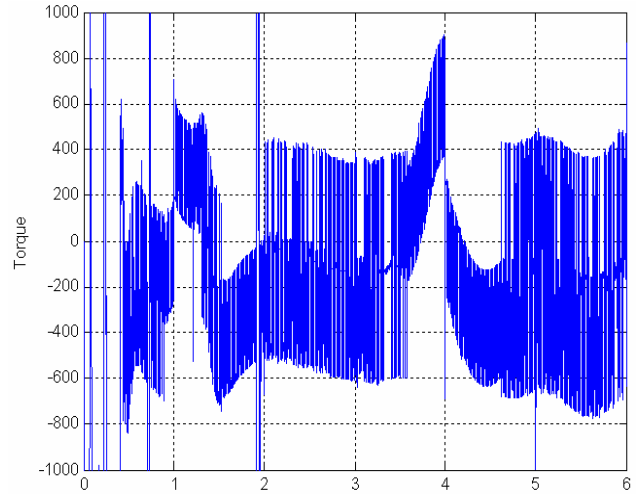


Figure 22. The torque signal  $u$  of left wheels with chattering phenomenon

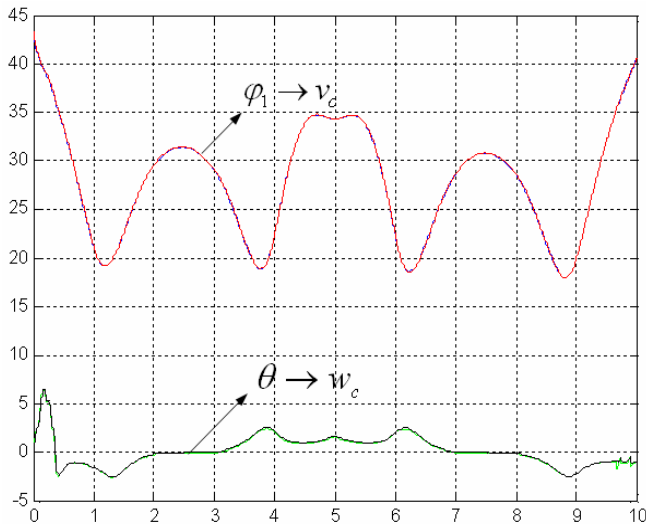


Figure 20. The trajectory tracking effect of privileged variable

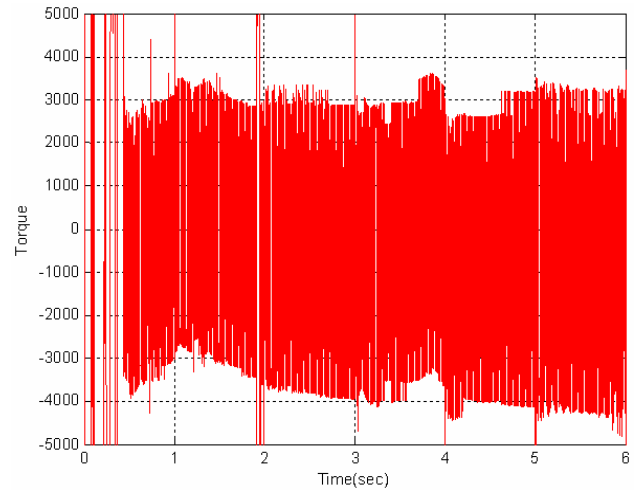


Figure 23. The torque signal  $u$  of right wheels with chattering phenomenon

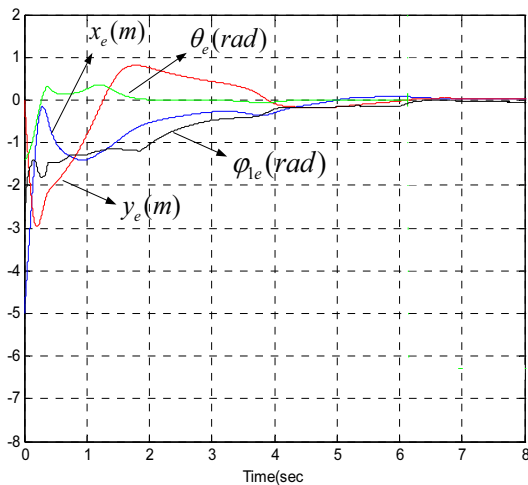


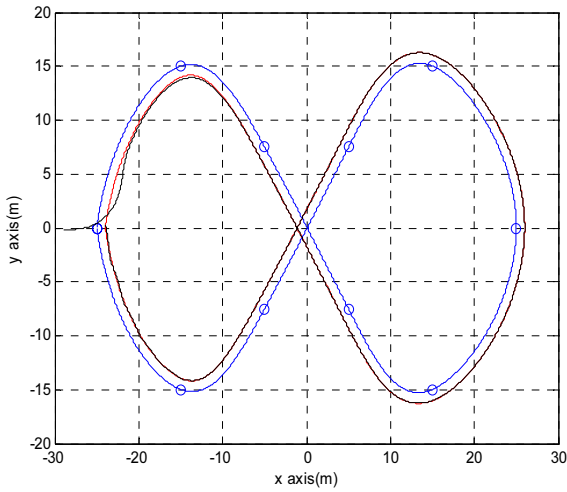
Figure 21. Tracking error of generalized variables

Figure 22 and Figure 23 are the torque signal  $u$  of left and right wheels with chattering phenomenon.

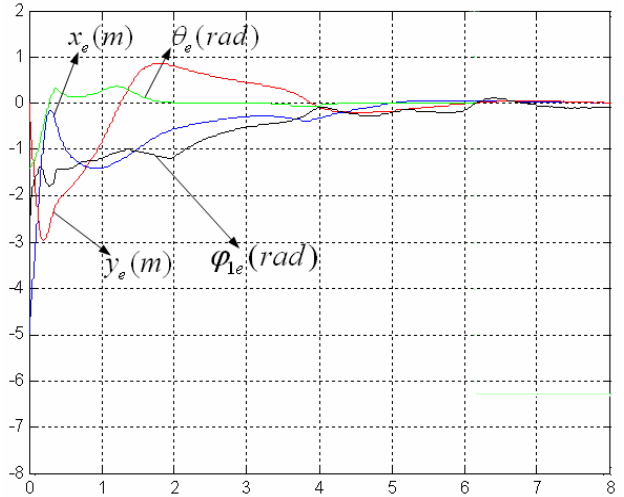
[Case V] Follow the previous example, using the FCMAC controller with smooth robust term to overcome the chattering problem

$$\begin{aligned}
 \mathbf{u} &= (\mathbf{G})^{-1} \left[ -\bar{\mathbf{f}} - \hat{\mathbf{f}} + \mathbf{y}_d^{(r)} + \Lambda^T \mathbf{e} + \mathbf{u}_r \right] \\
 \hat{\mathbf{f}} &= \hat{\mathbf{f}}(\mathbf{x} | \mathbf{w}) \\
 \dot{\hat{\mathbf{f}}}_i &= \Phi_{f_i} \mathbf{w}_{f_i}, \dot{\mathbf{w}}_{f_i}^T = -\gamma_{f_i} \mathbf{e}_i^T \mathbf{P}_i \mathbf{b}_i \Phi_{f_i}, i=1,2 \\
 u_{r_i} &= \hat{E}_i \cdot \text{sat}_B(\mathbf{e}_i^T \mathbf{P}_i \mathbf{b}_i), \text{ where} \tag{78} \\
 \text{sat}_B(\mathbf{e}_i^T \mathbf{P}_i \mathbf{b}_i) &= \begin{cases} \text{sgn}(\mathbf{e}_i^T \mathbf{P}_i \mathbf{b}_i), & |\mathbf{e}_i^T \mathbf{P}_i \mathbf{b}_i| > B \\ \frac{\mathbf{e}_i^T \mathbf{P}_i \mathbf{b}_i}{B}, & \text{otherwise} \end{cases} \\
 \dot{\mathbf{w}}_{f_i}^T &= -(\gamma_{f_i} \mathbf{e}_i^T \mathbf{P}_i \mathbf{b}_i \Phi_{f_i} + \sigma_{f_i} \mathbf{w}_{f_i}^T) \\
 \dot{\hat{E}}_i &= \gamma_{e_i} |\mathbf{e}_i^T \mathbf{P}_i \mathbf{b}_i| - \sigma_{e_i} \hat{E}_i
 \end{aligned}$$

The blue and red are the desired B-spline curve of left and right wheels of 3-wheel mobile robot in Figure 24, and the shaded block line shows the tracking performance in Figure 25.

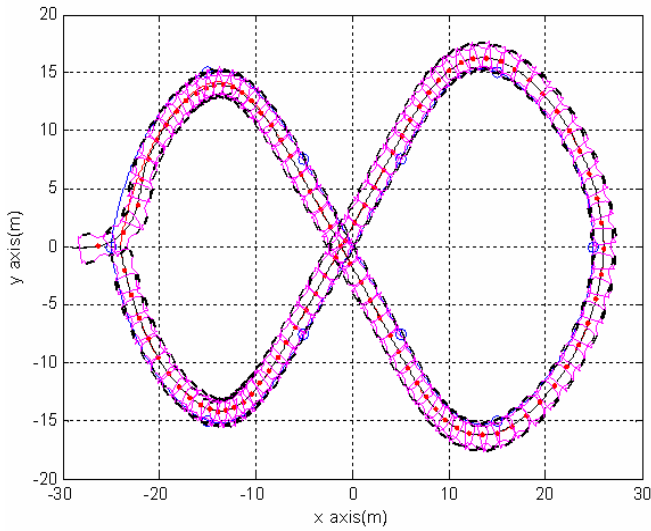


**Figure 24.** The desired B-spline curve of left and right wheels of 3-wheel mobile robot



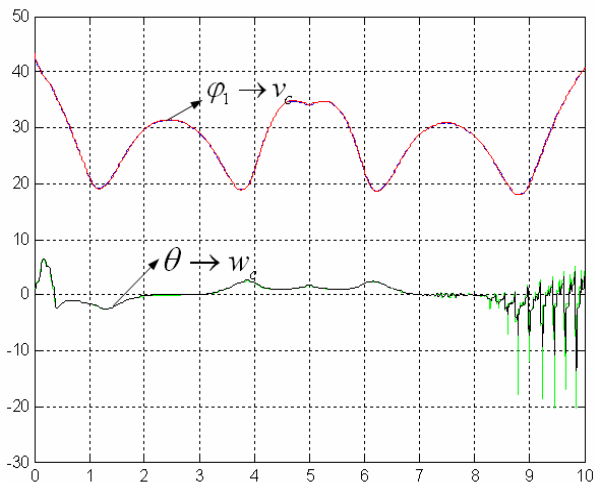
**Figure 27.** Tracking error of generalized variables

Figure 28 and Figure 29 are the torque signal  $u$  of left and right wheels to overcome chattering problem.



**Figure 25.** The trajectory tracking performance

Figure 26 illustrate the trajectory tracking effect of privileged variable and tracking error of generalized variables show in Figure 27.



**Figure 26.** The trajectory tracking effect of privileged variable

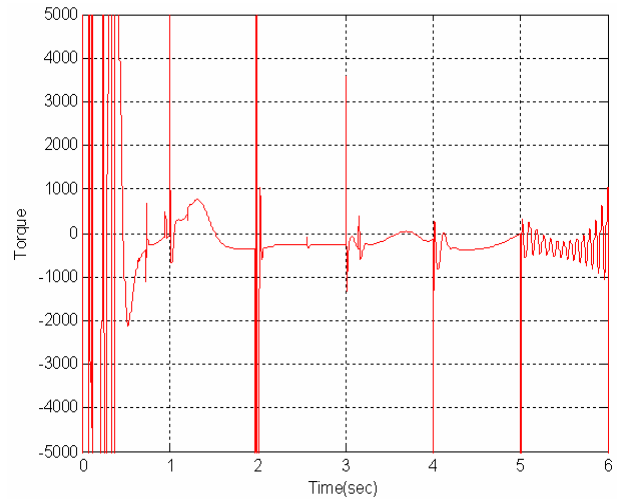


**Figure 28.** The torque signal  $u$  of left wheels to overcome chattering problem

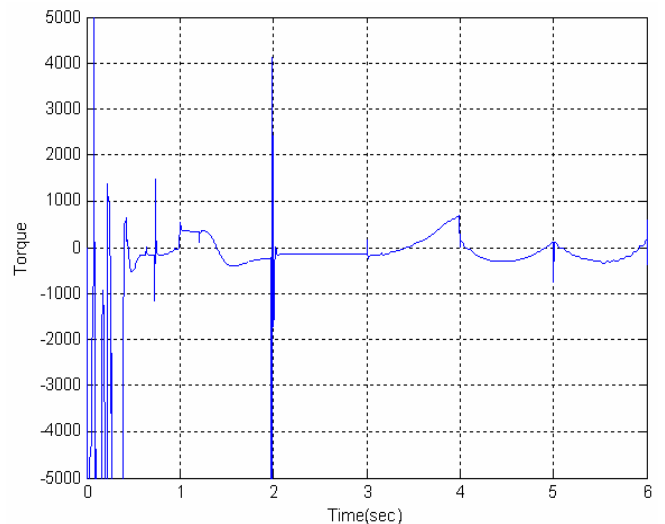


**Figure 29.** The torque signal  $u$  of right wheels to overcome chattering problem

